

## Article

# Generation and Transmission Expansion Planning: Nexus of Resilience, Sustainability, and Equity

Dahlia Byles <sup>1</sup>, Patrick Kuretich <sup>2</sup> and Salman Mohagheghi <sup>1,\*</sup> <sup>1</sup> Electrical Engineering Department, Colorado School of Mines, Golden, CO 80401, USA; drbyles@mines.edu<sup>2</sup> Xcel Energy, Denver, CO 80202, USA

\* Correspondence: smohaghe@mines.edu

**Abstract:** The problem of power grid capacity expansion focuses on adding or modernizing generation and transmission resources to respond to the rise in demand over a long-term planning period. Traditionally, the problem has been mainly viewed from technical and financial perspectives. However, with the rise in the frequency and severity of natural disasters and their dire impacts on society, it is paramount to consider the problem from a nexus of resilience, sustainability, and equity. This paper presents a novel multi-objective optimization framework to perform power grid capacity planning, while balancing the cost of operation and expansion with the life cycle impacts of various technologies. Further, to ensure equity in grid resilience, a social vulnerability metric is used to weigh the energy not served based on the capabilities (or lack thereof) of communities affected by long-duration power outages. A case study is developed for part of the bulk power system in the state of Colorado. The findings of the study show that, by considering life cycle impacts alongside cost, grid expansion solutions move towards greener alternatives because the benefits of decommissioning fossil-fuel-based generation outweigh the costs associated with deploying new generation resources. Furthermore, an equity-based approach ensures that socially vulnerable populations are less impacted by disaster-induced, long-duration power outages.

**Keywords:** capacity expansion planning; energy equity; energy justice; generation and transmission expansion planning; generation expansion planning; resilience; social vulnerability; sustainable power grids; transmission expansion planning



**Citation:** Byles, D.; Kuretich, P.; Mohagheghi, S. Generation and Transmission Expansion Planning: Nexus of Resilience, Sustainability, and Equity. *Processes* **2024**, *12*, 590. <https://doi.org/10.3390/pr12030590>

Academic Editors: George J. Tsekouras and Fotios D. Kanellos

Received: 20 February 2024

Revised: 9 March 2024

Accepted: 10 March 2024

Published: 15 March 2024



**Copyright:** © 2024 by the authors. Licensee MDPI, Basel, Switzerland. This article is an open access article distributed under the terms and conditions of the Creative Commons Attribution (CC BY) license (<https://creativecommons.org/licenses/by/4.0/>).

## 1. Introduction

The electric power grid must go through regular capacity expansions and upgrades to respond to the continuous increase in electric demand due to population rise and the higher utilization rate of electric loads. In recent years, the electrification of the transportation fleet has added a new challenge as utilities must now grapple with the expected electric vehicle (EV) charging demand, which will introduce additional stress on grid assets. Capacity expansion planning is often performed as generation expansion planning (GEP), transmission expansion planning (TEP), or a combination of both [1] and is formulated as a constrained optimization problem. One of the main objectives is to minimize the cost of grid expansion, which could include the cost of investment, operation, and maintenance [2–16]. The authors of [9,16] also included maximization of the salvage value as one of the objectives, which reflects the value of the installed resources at the end of the planning horizon. Penalties associated with imbalances between load and generation [15] or the cost of load shed [5,7,11,13] can also be considered. The authors of [17] investigated network improvement against seismic hazards and, in addition to the cost of generation and transmission enhancement, included the costs associated with repairs. Improvement in system reliability, for instance, in the form of minimizing the interrupted load and/or energy not served, has also been considered as an objective [3,10]. The GEP/TEP optimization model is solved subject to a variety of constraints. The most general constraints considered in the literature are the

overall load balance and node power balance equations, DC power flow and line flow limits, and limits on generation capacity [2–5,7,9–16]. Other constraints to model can be limits on the investment budget [2,12,14], commissioning time and installation constraints [9,18], fuel demand [2,4,14], and fuel transportation constraints [14]. Some have also incorporated constraints such as the prevention of islanding [4] or, conversely, enabling islanding by recommending the deployment of black-start-capable units, e.g., battery energy storage [7].

In the past decade, more researchers have been focused on integrating sustainability within the objectives of the grid expansion model. This has included limiting generation options to renewables, prioritizing renewable generation technologies over non-renewables, penalizing the deployment of transmission lines (which are known to have negative environmental consequences), and/or using life cycle assessments (LCAs) to weigh different options in terms of material use, human health impacts, and environmental impacts. A detailed review of the literature on sustainable grid expansion and models proposed in the literature appears in the authors' previous work in [19].

While traditional GEP/TEP models focus on normal contingencies and scenarios for generation and demand, the rise in the frequency and severity of natural disasters and their potential impact on the power grid's ability to meet overall demand have made it necessary to incorporate resilience into grid expansion planning. Power grid resilience focuses on how the grid responds to large-scale yet less-frequent events such as natural disasters. The high-impact, low-probability (HILP) nature of these events makes them different from the typical faults and disturbances that occur in power systems. There is no accepted standard definition for power system resilience. However, most researchers use the definition from the US Federal Energy Regulatory Commission (FERC), in which resilience is defined as "the ability to withstand and reduce the magnitude and/or duration of disruptive events, which includes the capability to anticipate, absorb, adapt to, and/or rapidly recover from such an event" [20]. Being able to withstand an event is further broken down into the ability to absorb its impacts and adapt to the changes caused by it [21]. The definition by CIGRE working group C4.47 introduces additional dimensions such as anticipation, preparation, absorption, sustainment of critically operated systems, swift recovery, adaptation, and implementation of the lessons learned from previous events [22]. In a more general context, the National Infrastructure Advisory Council (NIAC) has listed four attributes of a resilient system [23], namely, robustness, resourcefulness, rapidity, and adaptability. Strategies to improve grid resilience can be divided, based on their timeline, into three categories: preventative, corrective, and restorative. While corrective and restorative measures focus on operation strategies after the onset of the event, preventive measures are steps that utilities can take in preparation for a disaster event. These are usually performed during the design and expansion planning stage, which is the focus of the current paper. Typical preventive measures for bulk power grid resilience include reinforcing overhead line structures, hardening substations, and introducing network redundancy by adding lines and generators. Naturally, all these solutions require materially intensive facilities or equipment, which have a non-negligible impact on the environment and material resources. Hence, it can be argued that solutions for power grid infrastructural resilience may contradict grid sustainability, which further underlines the importance of finding a balance between these two critical design objectives.

Although technical and environmental dimensions of grid capacity expansion are undoubtedly important, the ultimate goal should be to maximize the benefits of those investments to society as a whole. This has gained more attention in recent years thanks, in part, to the major natural disasters that have left numerous residents without access to electricity for long periods of time. The literature shows that long-duration power outages impact socially vulnerable populations disproportionately [24]. Power system resilience studies have traditionally quantified outages using strictly reliability-centric metrics such as 'energy not served' or 'value of lost load'. This view, however, ignores the additional burdens that socially vulnerable populations face when dealing with disaster-induced outages and their capacity (or lack thereof) to respond to it. There has been considerable

new research quantifying how equity can be considered in power system planning studies against HILP events. For instance, Liu et al. considered equity by maximizing the fairness and efficiency of how electricity is rationed in a resiliency decision-making model [25]. Others have proposed equity-based models specific to distribution grid planning [26,27]. Montoya-Rincon et al. studied how infrastructure interdependencies can affect socially vulnerable populations during extreme weather events. Their model was developed for Puerto Rico [28] and quantified social vulnerability for power and water disruptions using an index from the Centers for Disease Control (CDC) which was augmented with additional socioeconomic factors. The authors in [28] claim that this work can be used to analyze how socially vulnerable communities will be affected by system resiliency upgrades. Gunda et al. developed a methodology to develop equity-based objective functions and inform equations for specific geographical locations and communities [29]. Various case studies throughout industries such as aviation, water usage, and microgrids were studied and showed the importance of getting stakeholders involved in any infrastructure upgrade to help alleviate burdens on socially vulnerable populations. More specific to long-duration power outages, the authors of [24] proposed a metric of social vulnerability based on the three dimensions of health (being at risk of detrimental health effects due to a long-duration power outage), preparedness (being unprepared for a long-duration power outage), and evacuation (a combination of evacuation intention and means, with people being most vulnerable when they intend to evacuate but face obstacles in doing so). A variety of socioeconomic and demographic factors were considered for each dimension. The authors then applied their model to all census tracts in Colorado to identify areas in which residents are most vulnerable to disaster-caused outages.

This paper proposes a novel approach to grid expansion planning based on the nexus of resilience, sustainability, and equity. The three objectives, which may, at times, be contradictory to one another, interplay in a risk-based environment (Figure 1). Resilience is modeled by considering the risk of wildfires, as one of the most common natural hazards in the state of Colorado. The contributions of the paper can be listed as follows:

- The proposed model for grid expansion finds a balance between (at times) opposing objectives of resilience, sustainability, and equity. A multi-objective model for grid expansion is proposed and solved using a goal programming approach to ensure that no objective dominates others and that the Pareto optimal solution is achieved.
- The consequences of outages are quantified using the social vulnerability index developed in [24] to weigh (prioritize) different demand nodes based on their perceived vulnerability levels. This can ensure that the improved grid resilience and energy not served will be balanced in favor of socially vulnerable populations. This prioritization of demand can be viewed as the *recognition justice* angle of energy equity, where the challenges and obstacles faced by individuals and communities in dealing with long-duration power outages are acknowledged and included in decision-making.
- The sustainability angle of grid expansion is modeled by quantifying the negative impacts of various generation technologies and transmission expansion options on resource usage, human health, and the environment. This is performed using an LCA-based analysis.

The rest of this paper is organized as follows: Section 2 discusses the problem formulation, including the objective functions and the associated constraints. Section 3 details the case study developed for a portion of the bulk power system in the state of Colorado. Section 4 presents the results and findings, followed by concluding remarks in Section 5 of the paper.

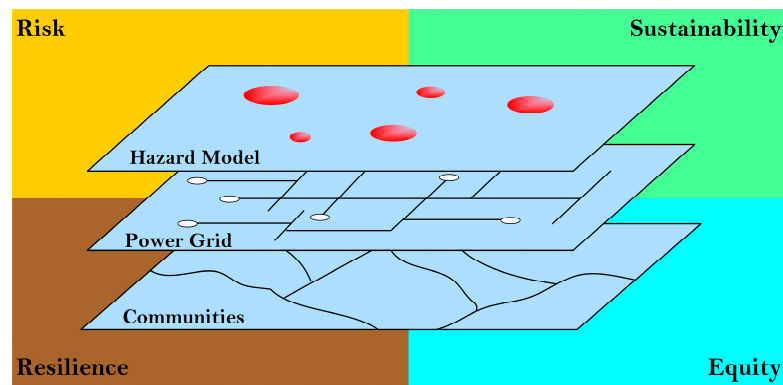


**Figure 1.** The proposed multidimensional grid expansion planning model considers the three objectives of maximizing resilience, maximizing sustainability, and maximizing equity, all within a risk-based framework. According to the expected utility theory, risk is modeled here as the probability of an event (loss of load) multiplied by its consequence.

## 2. Problem Formulation

This paper proposes a multi-objective optimization framework for generation and transmission capacity expansion, simultaneously considering resilience, sustainability, and equity. It is formulated as a linear risk-based, security-constrained, multi-objective optimization model that is solved subject to various operational constraints. Several assumptions have been made in the development of the problem formulation. First, the model is developed for a vertically integrated utility (VIU) that owns its transmission network and most of its generation. In addition, the candidate locations for possible generators and lines to be installed are assumed to be known. This is not unusual since most electric utilities typically have a clear understanding of where energy resources reside and how they should be connected to their existing grid. Next, it is assumed that only one generation technology can be deployed at each candidate node. This assumption has been made for ease of presentation and does not affect the generality of the developed model. Furthermore, as is the case in all grid expansion models, the annual load profile is assumed to be available, showing the system operating states, each with a corresponding load level and duration (in hours). For simplicity, it is assumed that all node loads follow the same pattern, as seen in Figure 2.

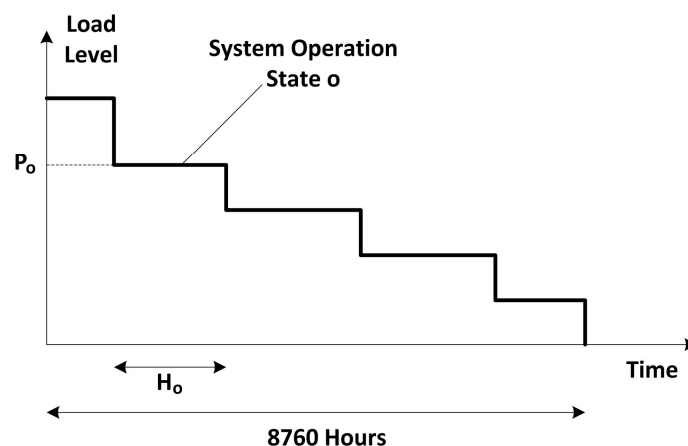


**Figure 2.** Representation of the operating states.

### 2.1. Objective Functions

The objective functions of the proposed multi-objective framework are defined as follows.

### 2.1.1. Minimize Energy Not Served

For every scenario  $s$ , within the set of scenarios  $S$ , the load not served should be minimized. The objective function (1) can be viewed as the expected energy not served (EENS), weighted by the social vulnerability levels of demand nodes to long-duration power outages, i.e.,  $\alpha_d$ . In this study, social vulnerability to long-duration power outages is quantified as the extent to which a person's life and livelihood is put at risk during a long-duration outage, as in [24]. By weighing loads based on their vulnerability levels, the objective function pushes towards a more equitable operation during normal and potential contingency scenarios.

$$\min \sum_{s \in S} \left( p_s \cdot \sum_{t \in T} \sum_{o \in O} h_o \cdot \left[ \sum_{d \in D} \alpha_d \cdot (P_{d,t,o,s}^{\text{des}} - p_{d,t,o,s}) \right] \right) \quad (1)$$

The probability that a scenario occurs is denoted  $p_s$ . The hour in the year is denoted as  $h_o$ . The energy not served is the difference between the desired demand  $P_{d,t,o,s}^{\text{des}}$  provided as the input to the model, and the actual energy supplied  $p_{d,t,o,s}$ . This is considered for every time step  $t$  within the planning period  $T$ , for every operating condition  $o$  within all operating conditions  $O$ , and for every demand node  $d$ .

### 2.1.2. Minimize Cost

This objective function includes both the capital costs associated with installing generators and transmission lines and the variable operation and maintenance (O&M) costs of both existing generators  $g$  and new (candidate) generators  $m$ . Capital and O&M costs can be calculated in a variety of ways that may differ from one utility to another. In this study, levelized cost of energy (LCOE) calculations conducted by the National Renewable Energy Laboratory (NREL) in their annual energy baseline were utilized [30]. The cost of installing new generators or lines is not a function of operating states, scenarios, or time. Also, notice that in this dynamic model, we allow the installed capacity  $p_{m,t}^{\text{max}}$  to be increased over the time horizon of the problem.

$$\min \left\{ \begin{array}{l} \sum_{s \in S_N} p_s \cdot \left( \sum_{t \in T} \sum_{o \in O} h_o \cdot \left[ \sum_{g \in G} (c_g^{\text{O\&M}} \cdot p_{g,t,o,s}) \right] + \sum_{t \in T} \sum_{o \in O} h_o \cdot \left[ \sum_{m \in M} (c_m^{\text{O\&M}} \cdot p_{m,t,o,s}) \right] \right) + \\ + \sum_{t \in T} \sum_{m \in M} (c^{\text{cap}} \cdot (p_{m,t}^{\text{max}} - p_{m,t-1}^{\text{max}})) \\ + \sum_{t \in T} \sum_{(i,j) \in L} ((u_{i,j,t} - u_{i,j,t-1}) \cdot c^{\text{line}} \cdot l_{i,j}) \end{array} \right\} \quad (2)$$

### 2.1.3. Minimize Life Cycle Impacts

Objective function (3) intends to minimize the life cycle impacts of the existing and candidate technologies. This LCA-based formulation is adapted from the work in [31]. Life cycle impacts are considered as variable impacts  $h_{c,tec}^{\text{var}}$  to model electricity production and transmission, and fixed impacts  $h_{c,tec}^{\text{fixed}}$  to model infrastructure construction. In this work, impact categories,  $C$ , from the ReCIPE 2016 report have been used, which include human health, ecosystem quality (freshwater and terrestrial), and resource scarcity [32]. OpenLCA [33] was then utilized to determine each generation technology's fixed and variable impacts. It characterizes each impact category into relative 'impact points' that can be used to compare the effects of each category. The variable impacts are divided by the fuel efficiency  $\eta_{g,\varphi}$  of the technology based on the generation type and the year the technology was commissioned. This is to account for the relative inefficiencies that occur as technologies get older depending on the type of plant. The fixed impacts are divided by the technology's lifetime  $\Lambda$  (in years) to spread the impact over the technology's entire lifetime rather than the initial construction year. More information on OpenLCA is detailed in Section 3.1.9.

$$\min \left\{ \begin{aligned} & \sum_{s \in S_N} p_s \cdot \left( \sum_{t \in T} \sum_{o \in O} h_o \cdot \left[ \sum_{g \in G} \sum_{c \in C} h_{c,tec}^{\text{var}} \frac{p_{g,t,o,s}}{\eta_{g,\varphi}} \right] + \sum_{t \in T} \sum_{o \in O} h_o \cdot \left[ \sum_{m \in M} \sum_{c \in C} h_{c,tec}^{\text{var}} \frac{p_{m,t,o,s}}{\eta_{m,\varphi}} \right] \right) + \\ & + \sum_{t \in T} \sum_{m \in M} (p_{m,t}^{\text{max}} - p_{m,t-1}^{\text{max}}) \cdot \left( \sum_{c \in C} \frac{h_{c,tec}^{\text{fixed}}}{\Lambda} \right) \\ & + \sum_{t \in T} \sum_{(i,j) \in L} l_{i,j} \cdot (u_{i,j,t} - u_{i,j,t-1}) \cdot \left( \sum_{c \in C} \frac{h_{c,tec}^{\text{fixed}}}{\Lambda} \right) \end{aligned} \right\} \quad (3)$$

## 2.2. Constraints

The above objective functions are optimized subject to the following constraints.

Active power must be balanced at all times, meaning that for each scenario, each operating condition, and at every time step the power generated must be equal to the power consumed, as seen in Equation (4).

$$\forall s \in S, \forall o \in O, \forall t \in T : \sum_{g \in G} p_{g,t,o,s} + \sum_{m \in M} p_{m,t,o,s} = \sum_{d \in D} p_{d,t,o,s} \quad (4)$$

Equation (5) presents the power flow constraint at each node. The sum of powers flowing out of each node for every scenario, operating condition, and time step must equal the sum of generation minus the demand at that node during the same scenario and operating condition.

$$\forall i \in N, \forall s \in S, \forall o \in O, \forall t \in T : \sum_{g \in G} p_{g,t,o,s} + \sum_{m \in M} p_{m,t,o,s} - \sum_{d \in D} p_{d,t,o,s} = \sum_{j \in N, j \neq i} p_{i,j,t,o,s} \quad (5)$$

The line flow constraints are modelled using DC power flow to ensure linearity throughout the model, as seen in Equations (6) and (7). This constraint consists of two sets, one for existing lines and another for candidate lines. For existing lines

$$\forall i, j \in N, (i, j) \notin L, \forall s \in S, \forall o \in O, \forall t \in T : p_{i,j,t,o,s} = b_{i,j} \cdot (\delta_{i,t,o,s} - \delta_{j,t,o,s}) \quad (6)$$

For candidate lines, the power flow constraint includes a binary decision variable  $u_{i,j,t}$  as to whether the line exists. The decision variable does not depend on the operating conditions or scenarios but considers time steps.

$$\forall i, j \in N, (i, j) \in L, \forall s \in S, \forall o \in O, \forall t \in T : p_{i,j,t,o,s} = b_{i,j} \cdot u_{i,j,t} \cdot (\delta_{i,t,o,s} - \delta_{j,t,o,s}) \quad (7)$$

It can be seen that Equation (7) consists of a bilinear term, which makes the model nonlinear. To ensure linearity of the model, this constraint is reformulated using the Big-K formulation proposed in [34] and shown in (8). Here, K is a large constant number. The selection of how large K should be is arbitrary. Planners should select a number that is larger than the power that could flow through the lines based on the maximum capacity of those lines. This is because Equation (15) limits the variable  $p_{i,j,t,o,s}$  to be within the maximum power handling capacity of the lines. In this study, K was set to 10,000. When the decision variable for a candidate line is 1, meaning that the line is chosen for deployment, the power flowing through the line equals the susceptance multiplied by the voltage angle difference across that line (based on DC power flow) as each side of the equality constraint must equal zero. When the decision variable is zero, i.e., the line is not chosen for deployment, the power flow through the line (which does not exist) is constrained to be zero by Equation (15) below.

$$\begin{aligned} & \forall i, j \in N, (i, j) \in L, \forall s \in S, \forall o \in O, \forall t \in T : \\ & -(1 - u_{i,j,t}) \cdot K \leq (p_{i,j,t,o,s} - b_{i,j} \cdot (\delta_{i,t,o,s} - \delta_{j,t,o,s})) \leq (1 - u_{i,j,t}) \cdot K \end{aligned} \quad (8)$$

Equation (9) ensures that candidate lines are only implemented after the first time step, i.e., not deployed during the first year.

$$u_{i,j,0} = 0 \quad (9)$$

Equation (10) maintains voltage angles within realistic operational limits.

$$\forall i \in N, \forall s \in S, \forall o \in O, \forall t \in T : -\pi \leq \delta_{i,t,o,s} \leq +\pi \quad (10)$$

The power generated by each existing or candidate generator must be within that technology's maximum and minimum capacity, albeit weighted by their availability factors. Equation (11) covers existing generators while Equation (12) is for new (candidate) generators. Note that the lower limit is only enforced for the existing generators. In (12), the maximum capacity for candidate generators is a variable to be optimized that must be within permissible capacities. The way this constraint is formulated helps ensure that a separate binary decision variable is not needed for candidate generation nodes. Equation (13) ensures that a new generator is not installed during the first time step as this is the original planning period with only the existing infrastructure. Furthermore, (13) ensures that installed generation capacity cannot decrease throughout the planning horizon.

$$\forall g \in G, \forall s \in S, \forall o \in O, \forall t \in T : P_{g,s}^{\min} \leq p_{g,t,o,s} \leq AV_{g,t,o,s} P_{g,s}^{\max} \quad (11)$$

$$\forall m \in M, \forall s \in S, \forall o \in O, \forall t \in T : 0 \leq p_{m,t,o,s} \leq AV_{m,t,o,s} p_{m,t}^{\max} \leq P_m^{\max} \quad (12)$$

$$\forall m \in M, \forall t \in T : p_{m,0}^{\max} = 0, 0 \leq p_{m,t-1}^{\max} \leq p_{m,t}^{\max} \quad (13)$$

The power flow through each line is also limited by the maximum capacity that the conductor can handle. Depending on the length of the line and the system's operating condition, this may be limited by the conductor's thermal rating or stability constraints. Similar to the above, two constraints are included, one for the existing lines (Equation (14)) and another for the candidate lines (Equation (15)). Equation (15) considers the decision variable for whether a line is deployed and ensures that the power flow across potential lines is constrained to zero when the line is not chosen for deployment by the model, i.e., when  $u_{i,j,t}$  is zero.

$$\forall i, j \in N, (i, j) \notin L, \forall s \in S, \forall o \in O, \forall t \in T : -P_{i,j,o,s}^{\max} \leq p_{i,j,t,o,s} \leq P_{i,j,o,s}^{\max} \quad (14)$$

$$\forall i, j \in N, (i, j) \notin L, \forall s \in S, \forall o \in O, \forall t \in T : -u_{i,j,t} \cdot P_{i,j,s}^{\max} \leq p_{i,j,t,o,s} \leq u_{i,j,t} \cdot P_{i,j,s}^{\max} \quad (15)$$

Equation (16) ensures that the model continues to implement and utilize a line if it was implemented in prior time steps.

$$\forall i, j \in N, (i, j) \notin L, \forall t \in T : u_{i,j,t} \geq u_{i,j,t-1} \quad (16)$$

Equation (17) ensures that, during normal scenarios, demand is always met. However, demand can be curtailed to help maintain the balance between load and generation during contingency scenarios, e.g., when a line or a generator may be experiencing an outage. This is expressed in Equation (18). Regardless, the level of curtailment is to be minimized (as enforced by Equation (1)).

$$\forall d \in D, \forall s \in S_N, \forall o \in O, \forall t \in T : p_{d,t,o,s} = P_{d,t,o,s}^{\text{des}} \quad (17)$$

$$\forall d \in D, \forall s \in \bar{S}_N, \forall o \in O, \forall t \in T : p_{d,t,o,s} \leq P_{d,t,o,s}^{\text{des}} \quad (18)$$

Finally, the decisions whether to implement candidate generation or lines are constrained by budgetary limitations, as seen in Equations (19) and (20).

$$\sum_{m \in M} c^{\text{cap}} \cdot p_{m,T}^{\text{max}} \leq B^{\text{gen}} \quad (19)$$

$$\sum_{(i,j) \in L} \sum_{t \in T} [(u_{i,j,t} - u_{i,j,t-1}) \cdot c^{\text{line}} \cdot l_{i,j}] \leq B^{\text{line}} \quad (20)$$

### 2.3. Solution Methodology

To find the optimal grid expansion strategy, objective functions (1)–(3) are minimized subject to constraints (4)–(6) and (8)–(20) using the Chebyshev goal programming methodology. The benefit of this approach is that it does not perform prioritization or weighting of objective functions, which would be subjective. Instead, each objective function is solved with respect to others to find the Pareto optimal solution. To achieve this, each objective  $q$  is first solved in isolation (subject to all relevant constraints) to find its true global optimum. Those optimal values are then set as targets  $T_q$  for the multi-objective model. The multi-objective model is then solved with the goal of minimizing the deviation of each objective function from its global optimum. This is performed by introducing deficiency variables  $s_q$ , which are to be minimized. The model is presented below.

$$\min L \quad (21)$$

Subject to:

$$\forall q \in Q : O_q - s_q \leq T_q \quad (22)$$

$$\forall q \in Q : \frac{s_q}{T_q} \leq L \quad (23)$$

$$\forall q \in Q : s_q \geq 0 \quad (24)$$

The objective function (21) can be viewed as minimizing the maximum deviation of all objective functions from their corresponding global optima. Constraint (22) allows each objective to exceed the target by a deficiency variable  $s_q$ , which is enforced to be positive per constraint (24). Equation (23) sets  $L$  to be the upper bound for the normalized deficiency variables. Normalization allows for comparing the objective functions to one another, despite the fact that each one may have values that are orders of magnitude different.

## 3. Case Study for Colorado

In this paper, a realistic case study is developed for the state of Colorado to demonstrate the applicability of the proposed methodology. All cases and scenarios have been built using publicly available data from the Public Service Company of Colorado (PSCO) and other public databases. Whenever public data were not available, reasonable assumptions were made to ensure that the system remains realistic. PSCO is a VIU that owns its generation, transmission, and distribution systems and also serves as the balancing authority. Using PSCO's generation and transmission network data simplifies the analysis as the regulatory market for power flow across transmission lines does not need to be considered. PSCO's electric resources and clean energy plan for 2021–2030 was used for the development of the case studies [35,36]. Therefore, the planning period utilized in all case studies spans from 2021 to 2030. The assessment of equity is based on a prior work by two of the authors, with a focus on Colorado [24].

### 3.1. Development of the Base Case

In this study, generation resources have been considered that are either owned by PSCO or have contracts with it and are integrated within its network. It should be noted that PSCO also has the option of importing energy via the market and uses this during peak load or when some units are down due to scheduled maintenance. However, this aspect

has not been considered in the current model. The transmission lines considered are at a 115 kV voltage level and above. Some of the lines are not owned by PSCO; however, they were necessary to consider in this analysis due to their interconnection with generation resources that PSCO owns, or has contracts with (these are the lines highlighted in orange in Figure 3). Nodes were defined as the locations of step-down transformers from 230 kV or above to 69 kV at the minimum [37]. PSCO divides its operations into various regions: Denver, Boulder, Front Range, Greeley, High Plains, Mountain, Northern, San Luis Valley, Western, and Pueblo [38]. In this analysis, the granularity of boundaries considered could only be at the county level. However, realistically, regions may be split within two or more counties. When that happens, the region is assigned to the county that it covers the most [39]. Nodes outside PSCO’s operation regions are not considered, except for generation resources utilized by PSCO. Information on existing generation was derived from [35,36,38]. Information on transmission lines was adopted from [40]. After the analysis above, a 73-bus system with 102 existing transmission lines and 46 existing generation resources was created. The finalized model can be seen in Figure 3.

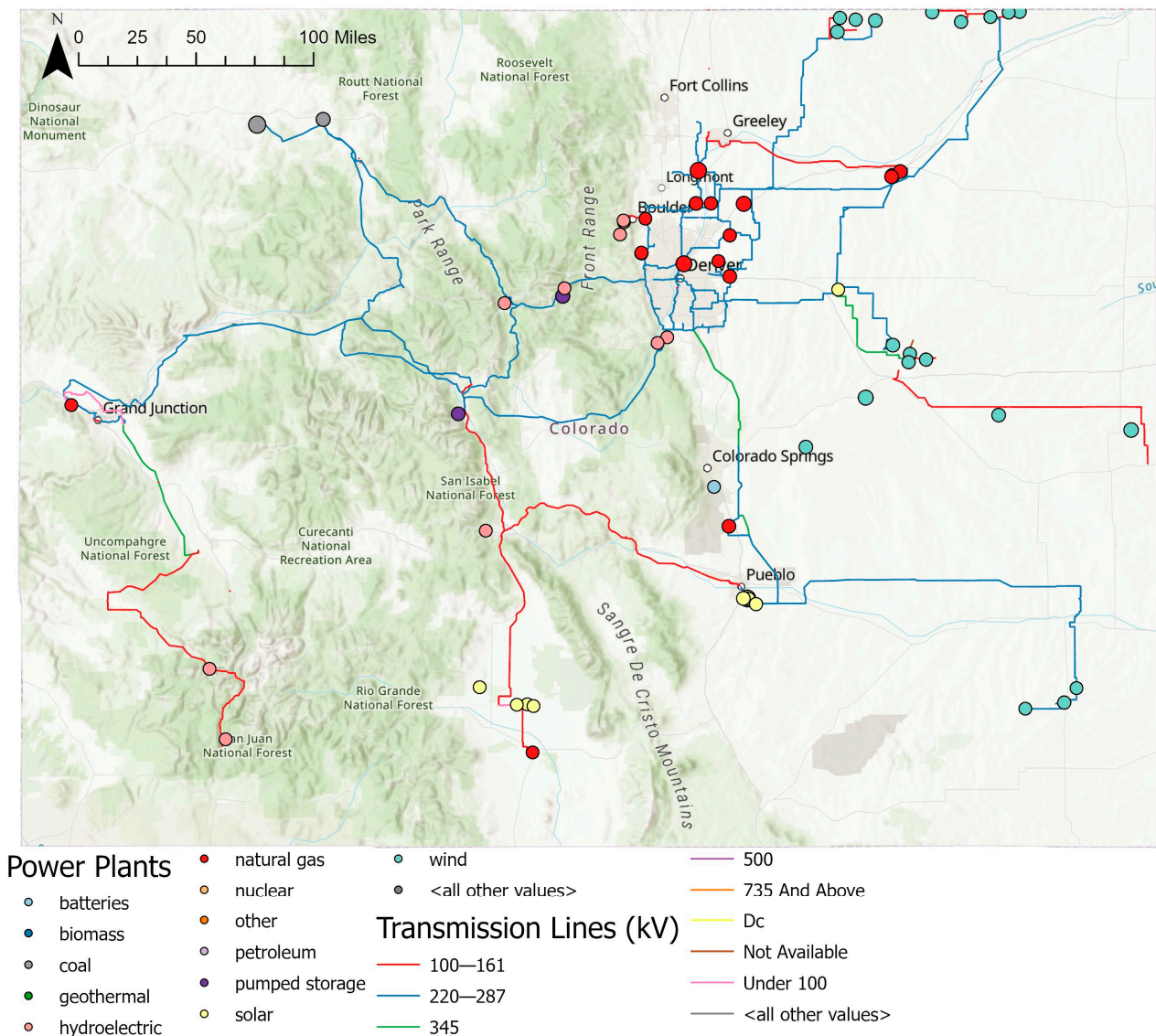


**Figure 3.** Finalized model for PSCO’s generation and transmission network. Data were obtained from [35–40]. The authors wish to emphasize that this is not a complete representation of PSCO’s network and has been developed for the purpose of this study.

### 3.1.1. Generation Resources

Reference [36] provides information on the type, maximum capacity (firm summer capacity), availability factor, and decommissioning year of each generation resource. The availability factors for purchased generation (not owned by PSCO) are not provided in [36] and are, therefore, estimated in this paper as the average of the availability factors of similar generation technology owned by PSCO. If a plant is decommissioned it has not been considered in the calculation of the average. For purchased generation, the decommissioning year was assumed to be the year that the power purchase agreement contract expired, which is provided in [36]. The general locations of generation resources were obtained from [38]. The year each generation source was commissioned was derived from [41]. The maximum capacity and the available capacity for the entire planning period are illustrated in Figure 4.

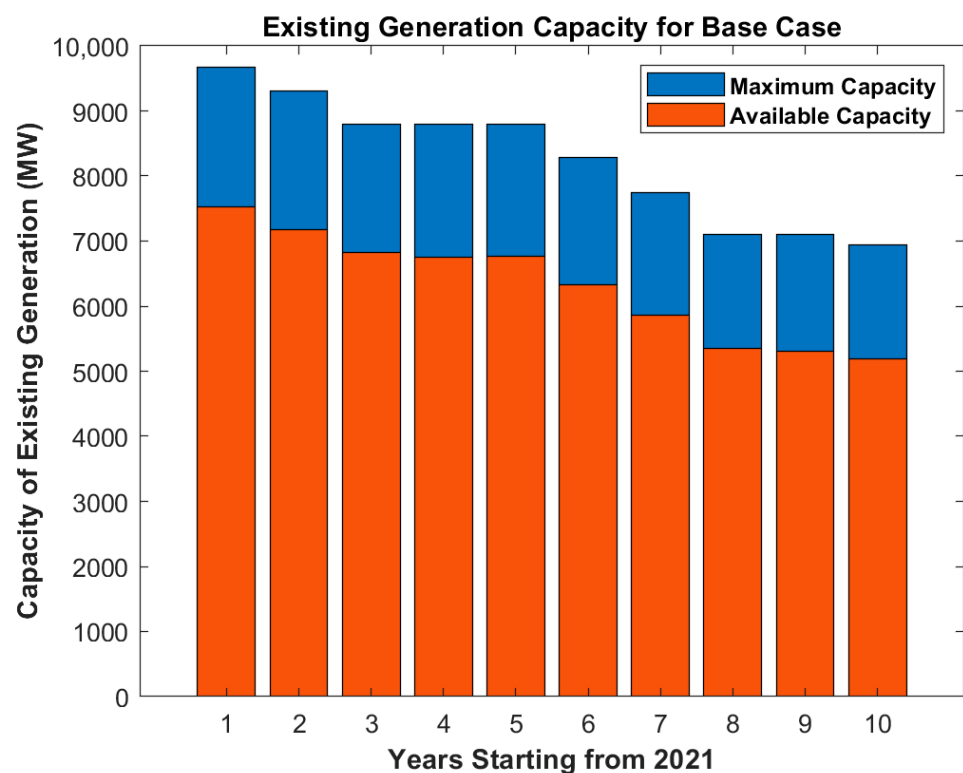


**Figure 4.** Existing generation capacity for the base case.

### 3.1.2. Transmission Lines

The parameters needed for existing transmission lines are length, susceptance, and maximum capacity. The length of each line was determined using the ArcGIS measure function. Conductors were assumed to be aluminum-conductor steel-reinforced (ACSR) and the same conductor types were assumed for each voltage level (see Table 1). A base power of 100 MW was considered in calculating the susceptance values per unit. If a transmission line consists of parallel lines, the overall susceptance value is adjusted accordingly.

**Table 1.** Conductor type considered for each voltage level [42–44].

Voltage Level (kV)	Assumed ACSR Conductor	Positive-Sequence Series Reactance (ohms/km)
115	Drake	0.337
230	Falcon	0.312
345	Plover	0.316

Without loss of generality, the maximum power handling capacity of each transmission line is calculated based on its voltage level, its positive-sequence series reactance per km, the length of the line, and a maximum phase angle difference of  $30^\circ$ .

$$P_{i,j}^{\max} = \frac{V_{line}^2 \sin(\delta_{max})}{x_{i,j} l_{i,j}} \quad (25)$$

In this study, we assumed that the maximum capacity of each line remains the same for each operating condition and each scenario. In practice, however, line capacities can be adjusted, for instance, according to their dynamic thermal rating.

### 3.1.3. Demand

The demand for each year was obtained from [36]. The retail peak demand was used as the demand for the first operating condition. The development of demand for all other operating conditions is described in Sections 3.1.6 and 3.1.7. A summary of customers served within each region, obtained from [45], is represented in Table 2. The Denver region is split into four sub-regions: Denver Metro, North Metro, Southeast Metro, and Southwest Metro. Without loss of generality, the number of customers in each sub-region was assumed to be a fourth of the total number of customers in the Denver region.

**Table 2.** Number and percentage of customers per region.

Region	Number of Customers	Percentage of Customers
Boulder	135,171	9.16%
Denver Metro	266,256.75	18.04%
Front Range	18,772	1.27%
Greeley	65,744	4.46%
High Plains	12,047	0.82%
Mountain	40,043	2.71%
North Metro	266,256.75	18.04%
Northern	39,120	2.65%
San Luis Valley	25,788	1.75%
Southeast Metro	266,256.75	18.04%
Southwest Metro	266,256.75	18.04%
Western	73,978	5.01%
Pueblo	0	0%

The percentage of total customers for each region was then allocated equally for each demand bus in that region. This percentage was utilized to determine how much of the total desired demand would be allocated to each bus. For instance, the Boulder region consists of 9.16% of the customers served. There are three buses in this region. Therefore, each bus requests 3.05% of the total demand for each operating condition. This representation can be seen in Figure 5.

The Northern region's demand was assigned to the two buses that are within the Greeley region. This was performed because, although lines extend into the Northern region from Greeley, those lines are not owned by PSCO, according to publicly available data, and, therefore, are not considered in this study.

### 3.1.4. Social Vulnerability Weighting

The social vulnerability of each demand node was determined using the data in [24], which provides the social vulnerability ranking for each census tract in the state of Colorado. Census-tract-level representation was too granular for the current study. Therefore, a weighted average social vulnerability score based on the population of each census tract was found and assigned to each county in Colorado. County populations were derived from [46]. All demand nodes within a county were assigned their county's respective social vulnerability score. The two nodes that supply the Greeley and Northern regions

are associated with two counties (Larimer and Weld); therefore, the average vulnerability score of those two counties was assigned to them. The overall social vulnerability levels are defined between 0 (least vulnerable) and 1 (most vulnerable). The results are illustrated in Figure 6.

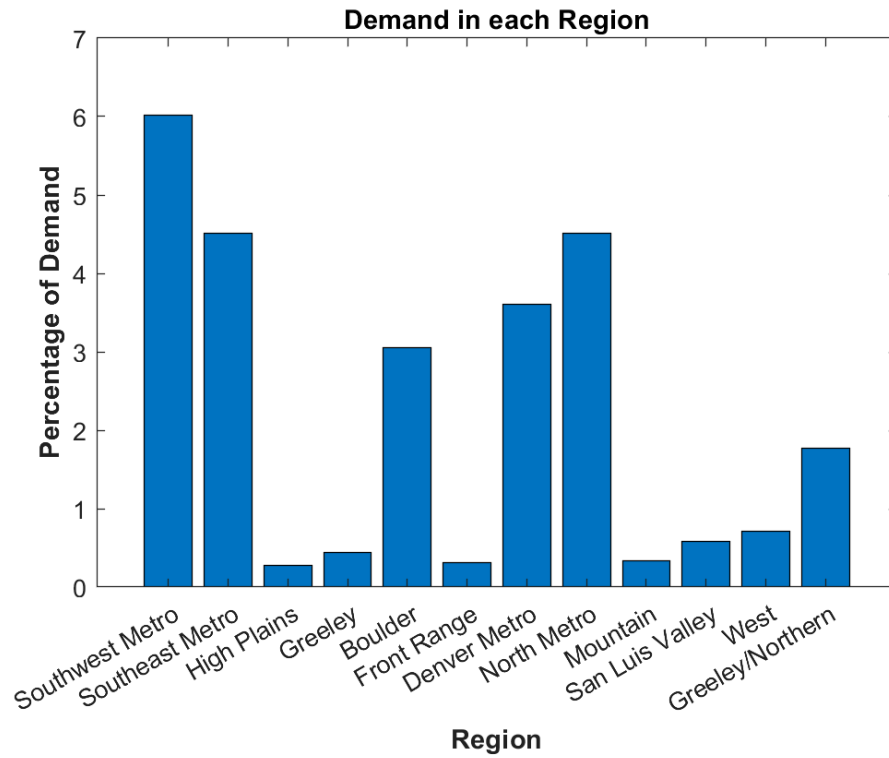


Figure 5. Total demand for nodes in each region.

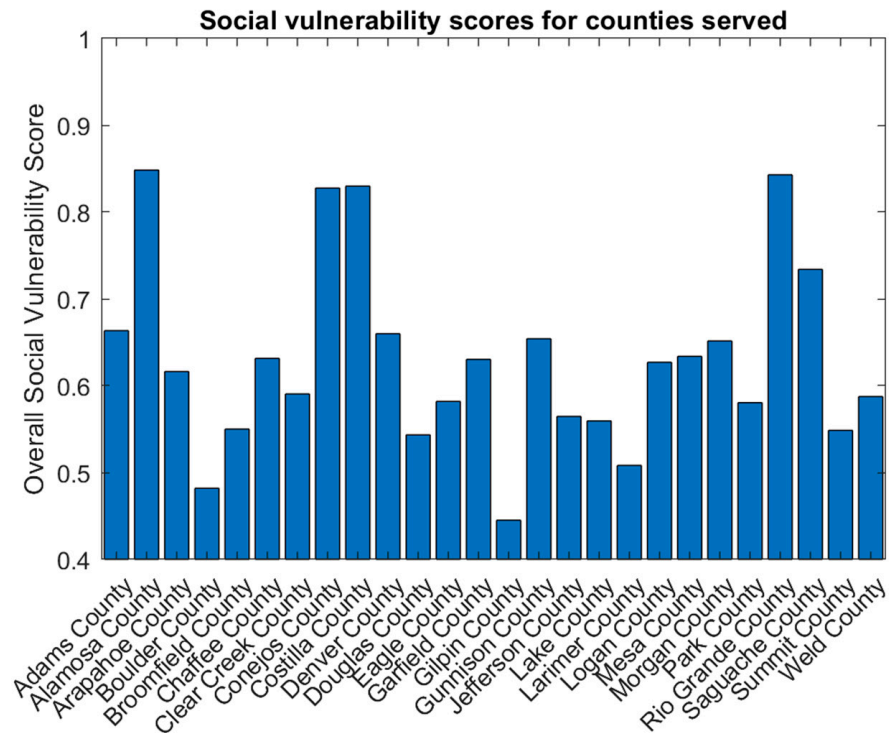


Figure 6. Social vulnerability to long-duration power outages of counties served.

### 3.1.5. Candidate Generation Resources and Transmission Lines

Between 2025 and 2026, PSCO’s peak demand is expected to exceed the existing generation capacity (see Figure 7) [36]. Therefore, generation resources must be added to the network to ensure that demand can be served at all times. The only candidate generation technologies considered in this study are wind and solar photovoltaic (PV) energy. The best area in Colorado for wind energy is in the eastern part of the state, with steady and robust wind conditions [47]. The best sites for solar PV energy resources are in southern parts of the state [48]. Western Colorado was also considered as a potential location for solar due to the need for additional generation in the western region. In this study, potential solar farms were allowed to be implemented at nodes 28 and 38 and potential wind farms at nodes 5, 44, and 45. The maximum capacity for all candidate generation resources was assumed to be 500 MW or greater. Adding generation resources may require building new transmission lines. PSCO is currently planning to construct various new transmission lines in eastern Colorado to allow for further integration of wind energy resources [49]. Furthermore, it was observed during the simulations that various transmission lines were operating at their maximum capacity for several operating conditions and scenarios. Those lines were, therefore, considered as candidates for additional reinforcement, perhaps by adding parallel circuits. All candidate transmission lines in this study are assumed to be at the 230 kV voltage level, with Falcon ACSR (see Table 3).

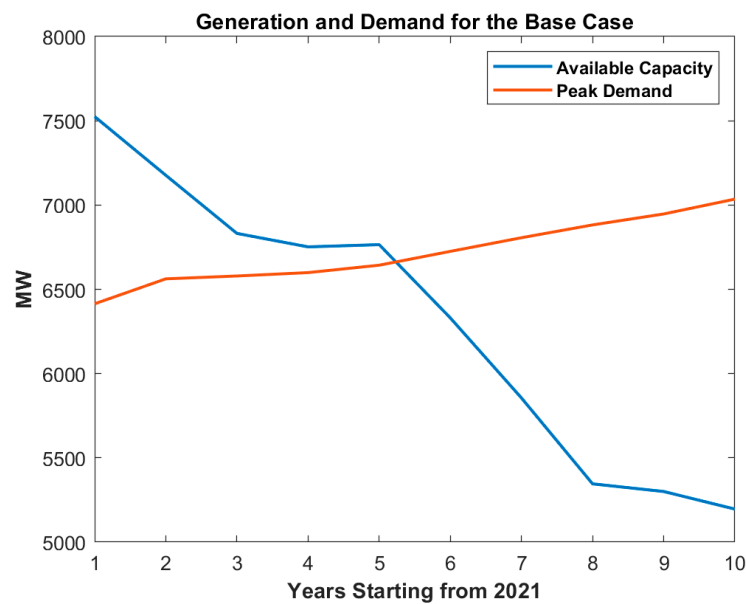


Figure 7. Available capacity of existing generation resources compared to peak demand for PSCO’s network. Available capacity and peak demand derived from [36].

Table 3. Specifications for candidate transmission lines.

From	To	Length (km)	Susceptance (p.u.)	Max Capacity (p.u.)
1	5	190	112.06	4.67
48	35	185	109.11	4.80
25	34	110	64.88	8.07

### 3.1.6. Operating Condition Development

To perform grid expansion studies, the annual demand needs to be divided into operating conditions (see Figure 2). There are different ways that utilities can accomplish this. In the absence of publicly available data from PSCO, an approximate approach was used in this paper. Operational seasons were determined as on-peak (June through

September) and off-peak (October through May), and four operating conditions were then defined as on-peak, average demand and above; on-peak, below-average demand, off-peak, average demand and above; and off-peak, below-average demand. To find the durations of these operating conditions, the annual energy delivered by PSCO from March 2022 to March 2023 was used (see Figure 8, data obtained from [50]). The peak daily demand was determined by dividing the peak energy consumption by 24 h and then used as the baseline for calculations. The demand (in MW) and number of hours for each one are listed in Table 4.

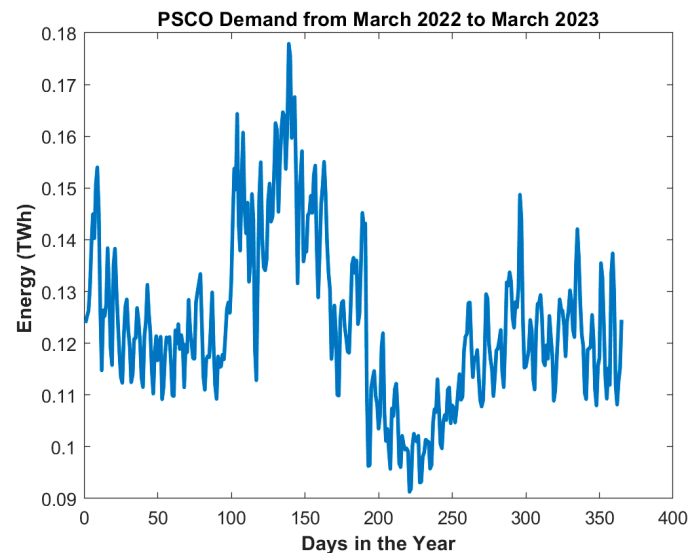


**Figure 8.** Energy delivered by PSCO from March 2022 to March 2023; data from [50].

**Table 4.** Operating condition specifications.

Operating Condition	Total Demand (MW)	Number of Hours
1: On-peak, average demand and above	6414.0	1368
2: On-peak, below-average demand	4558.7	1536
3: Off-peak, average demand and above	5553.0	2952
4: Off-peak, below-average demand	4248.9	2904

### 3.1.7. Scenario Development

Contingency scenarios were developed based on the risk of wildfires to communities, using a burn probability for the state of Colorado [51], which can be seen in Figure 9. The USDA Forest Service defines the probability of burn as “the likelihood that a wildfire will burn a given point” [52]. The burn probability quantifies the likelihood that a wildfire could occur. This is the ‘probability of the event’ that is reflected in the notion of risk. The intensity of a wildfire can also contribute to the potential that an asset may be damaged; however, this aspect is not considered in the current study.

The Front Range has the highest burn probability in the entire state. Any line or generator with a burn probability of 0.1% (1 in 1000 from the legend in Figure 9) or more was considered a potential contingency scenario. For this study, only (N – 1) contingencies were considered. A list of the chosen scenarios and their probability of occurrence are provided in Table 5. The probability of occurrence was determined based on the highest burn probability that each line passed through, based on the map in Figure 9 [51]. Not surprisingly, most contingencies considered represent line or generation outages in the Front Range and Boulder service regions. In addition, line outage contingencies were considered in the San Luis Valley and the Western regions.

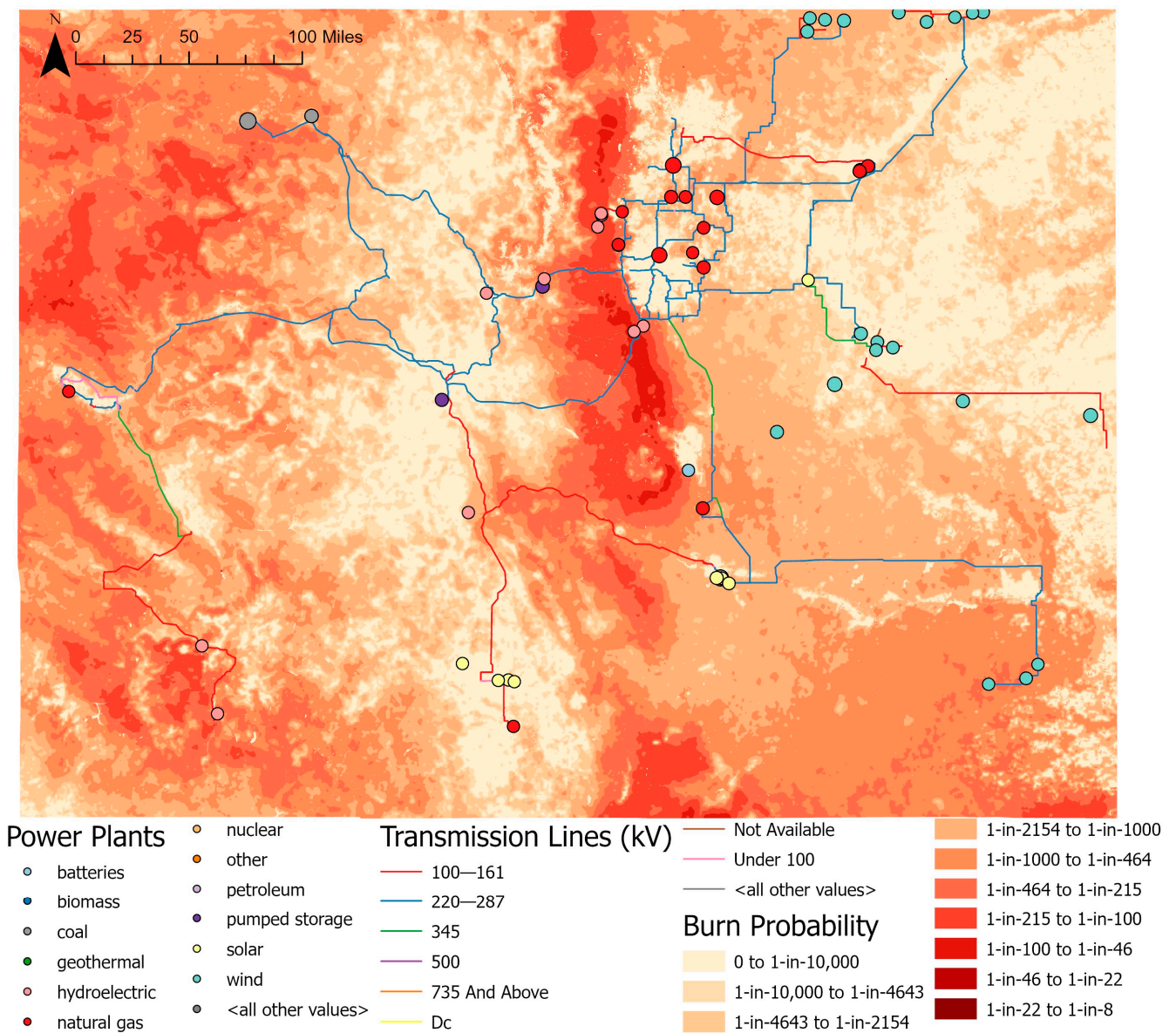


**Figure 9.** The probability of a burn for the state of Colorado overlaid on the case study network.

**Table 5.** Scenario descriptions.

Scenario	Description of Contingency	Probability of Occurrence Based on Burn Probability [51]
1	Line from 23 to 26 down	2.17%
2	Line from 26 to 27 down	1.00%
3	Line from 11 to 31 down	1.00%
4	Line from 35 to 37 down	0.47%
5	Line from 11 to 10	0.47%
6	Line from 11 to 25	1.00%
7	Line from 25 to 23	1.00%
8	Line from 2 to 23	0.47%
9	Generator at 31 (pumped hydro) down	0.47%
10	Normal Operation	91.97%

### 3.1.8. Cost and Budget

Data on capital costs and operation and maintenance costs for all generation technologies were obtained from the National Renewable Energy Laboratory’s annual energy

baseline [30] (see Figure 10). The capital cost to build one kilometer of a high-voltage transmission line was determined to be USD 2 million [49]. The budget for performing generation and transmission capacity expansion projects was considered in this study to be USD 2 billion each. This number was chosen for proof-of-concept purposes and is based on the budget that PSCO has defined to build the Colorado Power Pathway project [49]. Future PSCO grid expansion budgets may differ from that number.

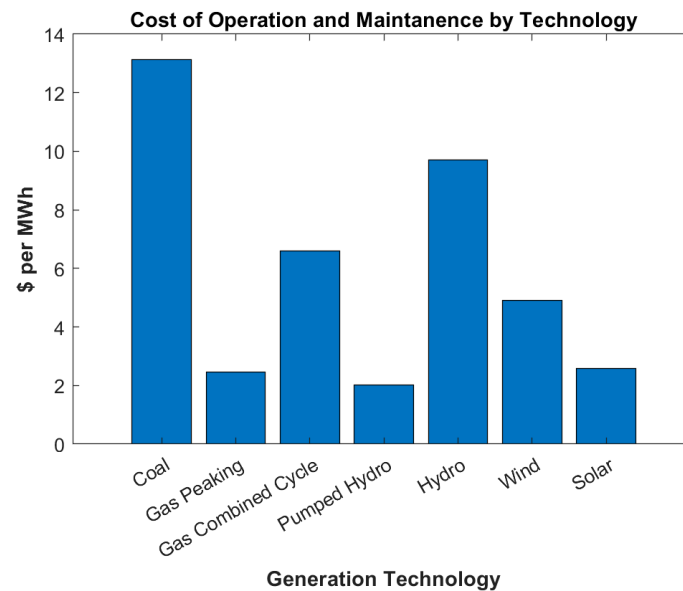


**Figure 10.** Cost of operation and maintenance for each generation technology considered.

### 3.1.9. Life Cycle Impacts

The fixed and variable environmental impacts of different expansion options were determined using OpenLCA V1.11.0, which is a professional life cycle impact assessment software [33]. It quantifies the fixed impacts into ‘points per power plant’ of the environmental impact indicator. To ensure proper units, the impact indicator is divided by the plant’s installed capacity. The overall fixed units considered are, therefore, ‘points per MW’. The fixed impact for the installation of transmission lines is in ‘points per km’. The variable environmental impacts are quantified as ‘points per MWh’ of environmental impact. The ReCiPe method was utilized as the life cycle impact methodology. It helps interpret the large number of results that a life cycle analysis can produce and breaks down the environmental effects into midpoint and endpoint environmental impact categories [32]. The three endpoint categories considered in this study are human health impacts, ecosystem quality impacts, and resource scarcity impacts. The energy storage units determined to be at nodes 68 and 70 in the model were assumed to have the same environmental impacts as solar PV plants because specific details on the impacts of energy storage technology were not available in OpenLCA. Pumped hydro storage plants were analyzed using OpenLCA data for pumped storage plants. The heuristic method was used, which considers impacts over a time horizon of 100 years. Efficiency factors were obtained from [31]. The impacts of different generation resources can be seen in Figure 11.

### 3.2. Aggravated Load Growth Case Study

In addition to the base case, a second case study was developed with aggravated load growth, where demands for the operating conditions were changed with respect to those of the base case. For the first operating condition, the data in [36] were used, where a roadmap scenario is provided starting from 2022, with the impacts of both electrification and electric vehicles considered. The rest of the operating conditions’ demands were determined using the same approach as defined above. A comparison of demand between the two cases is illustrated in Figure 12.

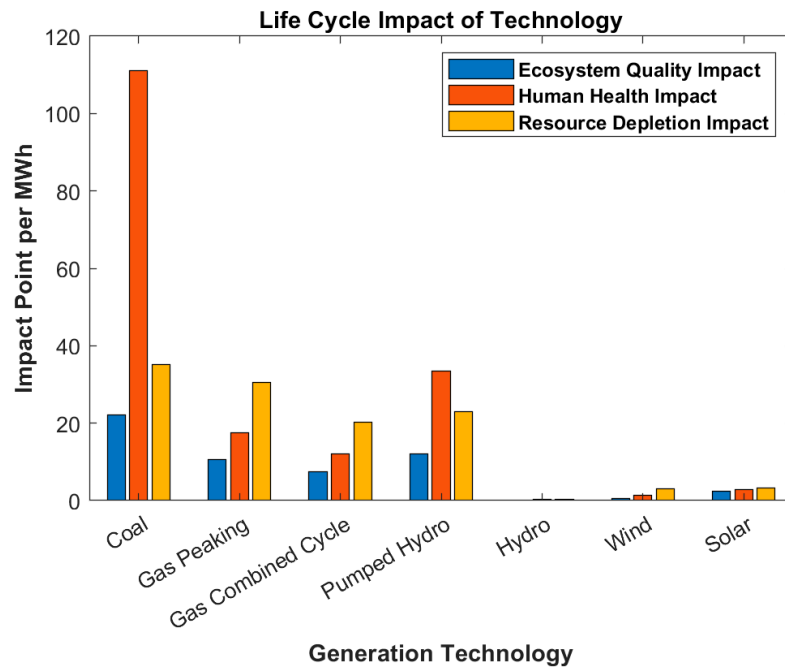


Figure 11. Life cycle impact by impact category for all generation technologies considered.

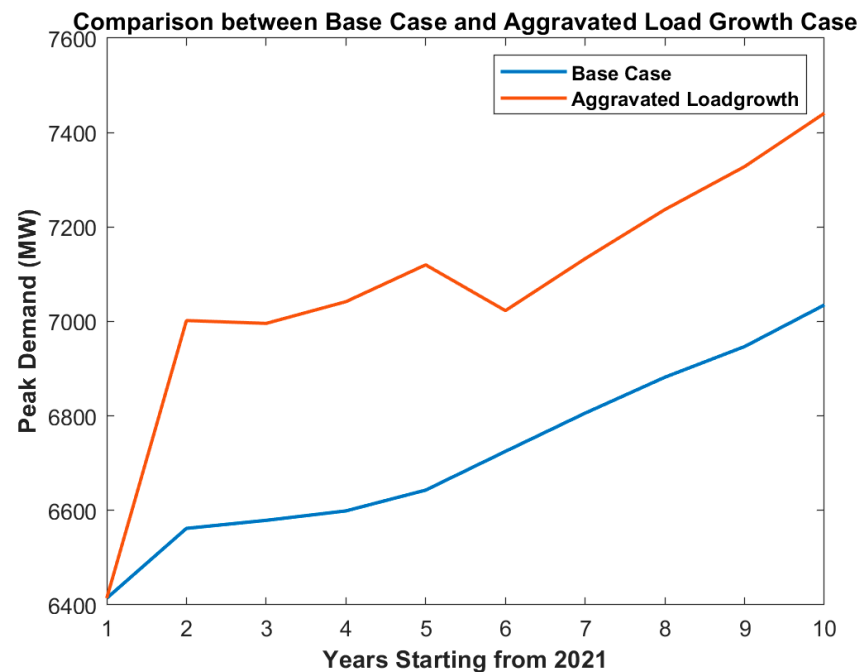


Figure 12. Comparison of demand between the base case and the aggravated load growth case.

### 3.3. Accelerated Decommissioning Case Study

A third case study was also developed considering the possibility of accelerated decommissioning. This was created by setting all the availability factors for any carbon-based generation technology to zero for 2027 and beyond. A comparison of the available generation capacity between the base case and the accelerated decommissioning case is illustrated in Figure 13.

Finally, a combined case study was developed with both aggravated load growth and accelerated decommissioning combined. This represents an extreme scenario characterized by higher demand and less non-renewable generation capacity.

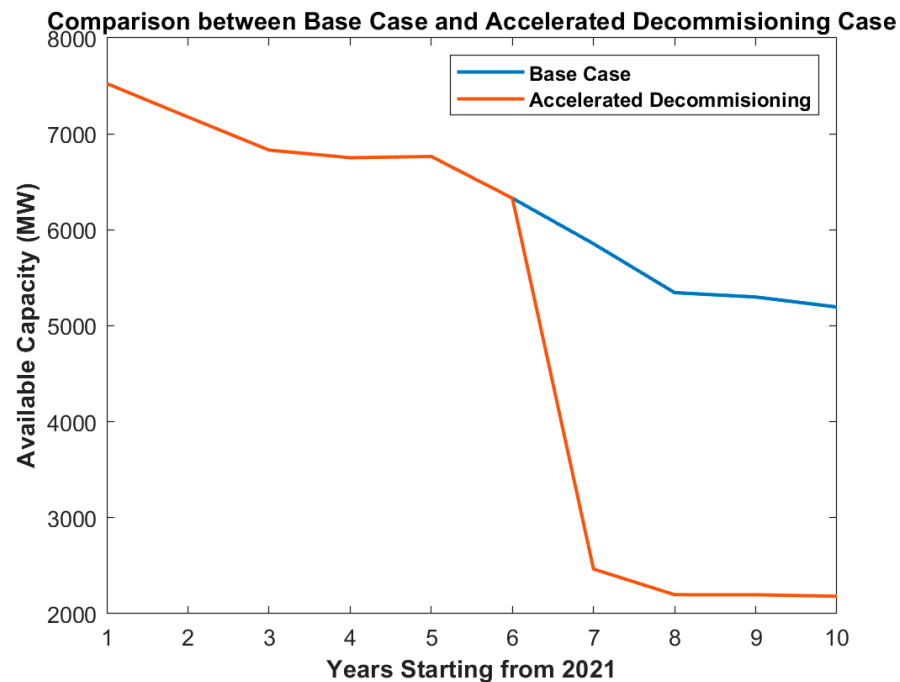


Figure 13. Comparison of available capacity between the base case and the decommissioning case.

#### 4. Results

The optimization model presented in Section 2 was solved for the case studies described in Section 3. These cases are labeled as base case, load growth, decommissioning, and both. The formulation was modeled in the Pyomo V6.7.1 software and solved using the Gurobi solver. For the given test system and on a computer with Intel® Core™ i7-8650U CPU @ 1.90 GHz, 2.11 GHz 16 GB RAM (Santa Clara, CA, USA), the optimization model converges in less than 5 min. To run the Chebyshev goal programming model, each objective function is first solved in isolation in order to determine its true global optimum, which are then used as the target values for the multi-objective framework. The single objective optima are reported in Table 6, and the results of the multi-objective model are presented in Table 7. All objective functions within the multi-objective framework failed to meet their single objective optima. This is expected as the weighted energy not served contradicts the other two objective functions. Therefore, it is not possible to achieve all goal (target) values simultaneously. However, using the Chebyshev goal programming methodology ensures that no objective function dominates others. It can be seen that the highest cost is related to the case with load growth and decommissioning (both). The decommissioning case also indicates the lowest life cycle impacts, as expected.

Table 6. Single objective optima for different case studies.

Objectives	Base Case	Aggravated Load Growth Case (Load Growth)	Accelerated Decommissioning Case (Decommissioning)	Aggravated Load Growth and Accelerated Decommissioning Case (Both)
Load Not Served (Weighted MW)	9674.25	9674.25	9674.25	9674.25
Cost (USD)	\$1,754,934,850.55	\$1,891,207,713.36	\$1,901,207,303.16	\$2,042,999,345.44
Life Cycle Impacts (Impact Points)	3,964,499,789.53	4,075,534,278.06	3,964,499,789.53	4,075,534,278.06

As expected, the cost of the base case, with no aggravated load growth and no accelerated decommissioning, is the lowest among all four cases. The case study that costs the most is the one with both load growth and decommissioning. Furthermore, the de-

commissioning case was costlier than the one with load growth alone. This is because more candidate generation resources had to be constructed in the former, leading to more capital costs. The pattern of life cycle impacts was slightly different from that of cost. Not surprisingly, the decommissioning case resulted in the lowest impacts. On the other hand, the case with both load growth and decommissioning resulted in the highest life cycle impacts, due to the deployment of new generation plants to respond to the growth in load and also replace the existing non-renewable ones.

**Table 7.** Multi-objective optima for different case studies.

Results	Base Case	Aggravated Load Growth Case (Load Growth)	Accelerated Decommissioning Case (Decommissioning)	Aggravated Load Growth and Accelerated Decommissioning Case (Both)
Maximum Deviation	0.238660266	0.225637015	0.233238455	0.231422596
Load Not Served (Weighted MW)	11,983.19	11,857.20	11,930.74	11,913.17
Cost (USD)	\$2,173,768,069.18	\$2,317,934,176.84	\$2,344,641,957.11	\$2,515,795,558.27
Life Cycle Impacts (Impact Points)	4,910,668,364.71	4,995,125,667.70	4,889,173,595.13	5,018,705,002.15

The optimal values for the weighted load not served did not change significantly between the four case studies. The case study with accelerated load growth showed the lowest amount of weighted load not served, in part due to the additional generation capacity built. Interestingly, this case also had the most significant ‘unweighted’ amount of load not served. This shows that although more of the load remains unserved in this case study, when weighted based on social vulnerabilities, more of the demand is covered, ensuring that it serves the most vulnerable populations during contingency scenarios.

#### 4.1. Comparison of Case Studies over Time

Figure 14 depicts the life cycle impacts over time for the base case and the load growth case. For easier assessment, the impacts of existing and added generation resources are shown separately. In both cases, the model reduces the output of the coal-fired power plant in year 2 (to almost zero) because of its high life cycle impacts. To replace its production, new wind and solar resources are added to the system, as shown by the increase in life cycle impacts associated with the added generation. This happens due to the multi-objective nature of the model, i.e., the increased cost due to installation of new wind and solar resources is balanced against the significant reduction in life cycle impacts associated with the coal plant. This is depicted from a different perspective in Figure 15, which shows the drop in generation of existing resources (i.e., the coal-fired power plant) and an increase in power generation and generation capacity associated with new resources.

#### 4.2. Assessment of Individual Technologies

The model did not implement any new transmission lines for any case study. However, new generation resources were implemented. Figures 16 and 17 illustrate the life cycle impact points and power generation associated with each type of generation resource (existing and added) for the base case. Naturally, coal, combined cycle, and gas peaking plants all produce a considerable number of impact points during the initial planning year. The model does not allow new construction until the second planning year. Therefore, the first-year impacts most accurately represent the current potential impacts from Colorado’s electrical infrastructure. The model then heavily constricts these polluting sources (due to its multi-objective nature) and implements generation technologies with lesser impacts. After the initial planning year, the added solar generation has the most impacts, except for planning year nine, where impacts associated with the combined cycle plant increase. Figure 17 shows that, although the added generation capacity of wind and solar is con-

siderably more than that of coal during the initial planning period, the impact of these technologies is significantly less than that of coal.

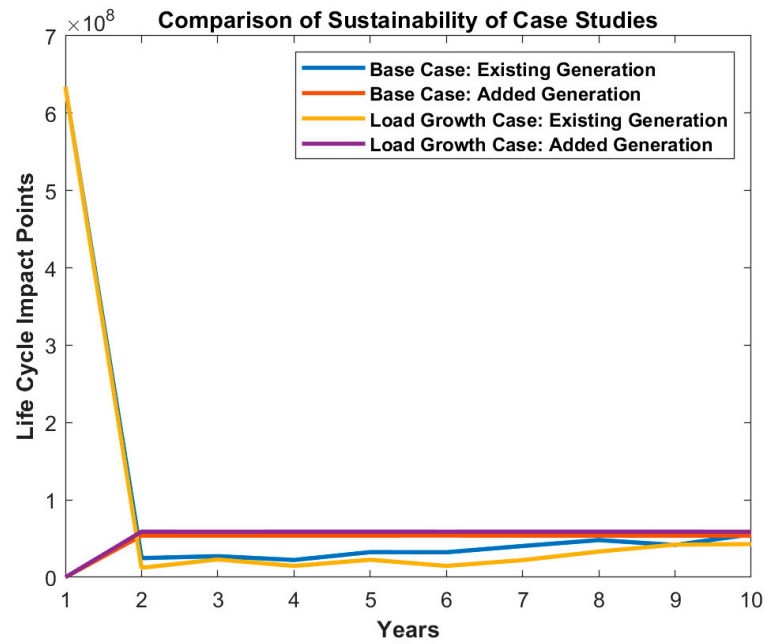


Figure 14. Comparison of life cycle impacts over time between the base case and the load growth case.

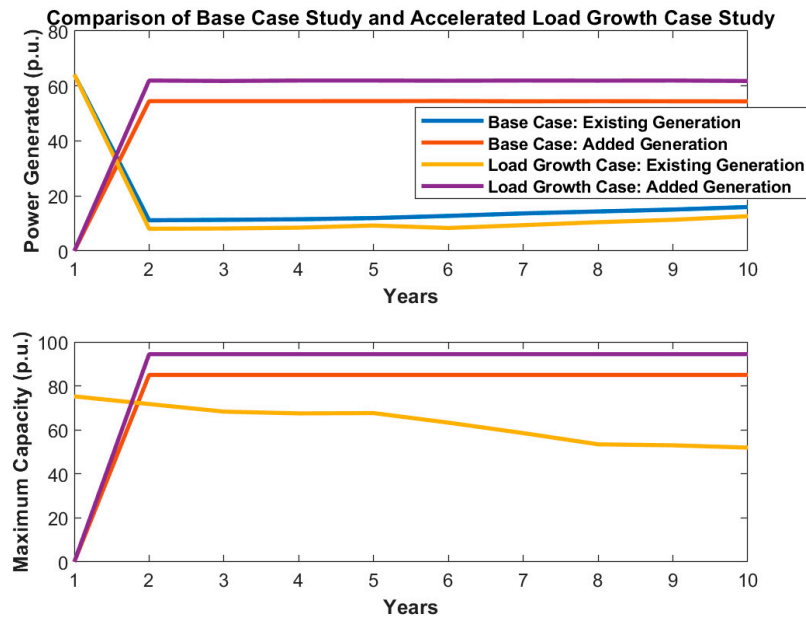


Figure 15. Comparison of power generated and maximum capacity between the base case and the load growth case.

Figure 18 shows the power generation levels of each generation technology at each bus, throughout the planning period, for the base case. Normal operation is considered (i.e., no contingency scenarios) with above-average demand. For better visualization, two graphs are provided, one with the existing generation (top) and another with both existing and added generation (bottom). It can be seen that generation by the added resources dominates that of the existing units at several buses. The model heavily curtails coal, combined cycle, and gas peaking plants for the first few years. In later years, after more load growth is experienced, the gas peaking and combined cycle plants start to generate more power. Interestingly, generation by energy storage decreases. This is in part due

to the higher life cycle impacts of the unit (pumped hydro storage at bus 31) compared to renewable technologies. The lower graph in Figure 18 shows that the model adds a significant amount of wind and solar resources. This is consistent with the environmental impact points found in Figure 16.

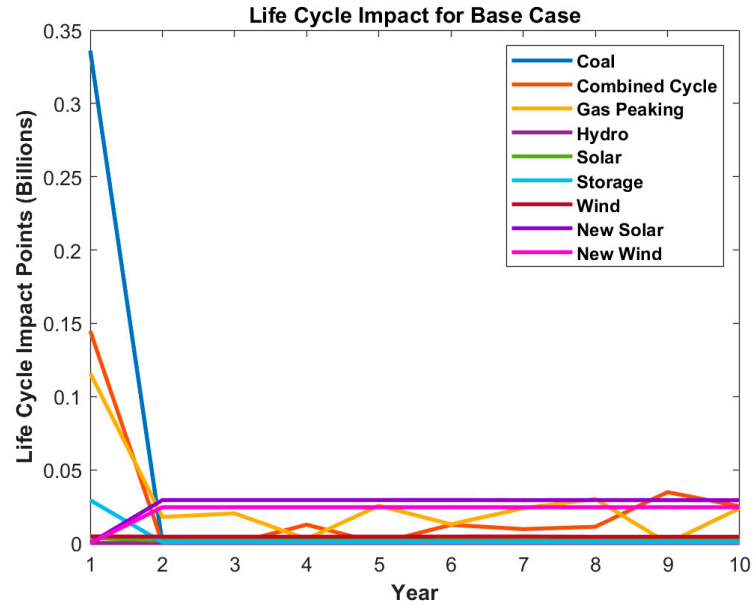


Figure 16. Life cycle impacts during the planning period for the base case.

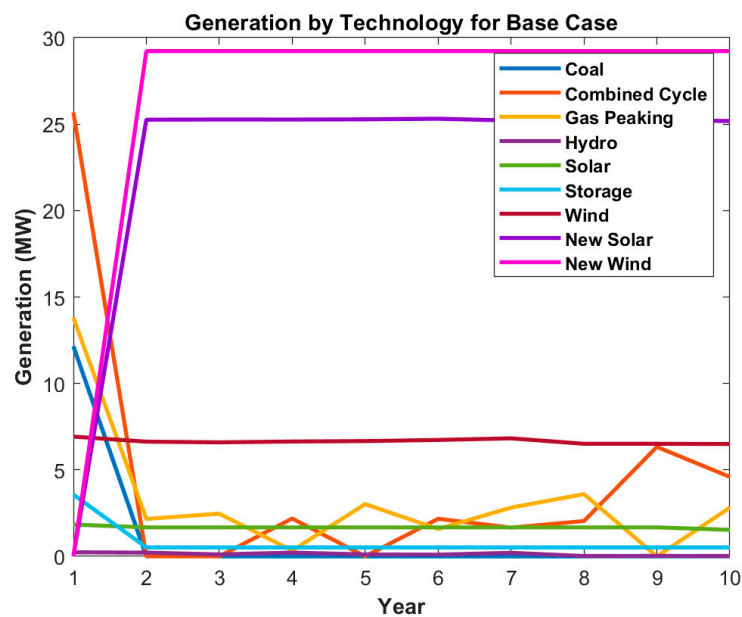
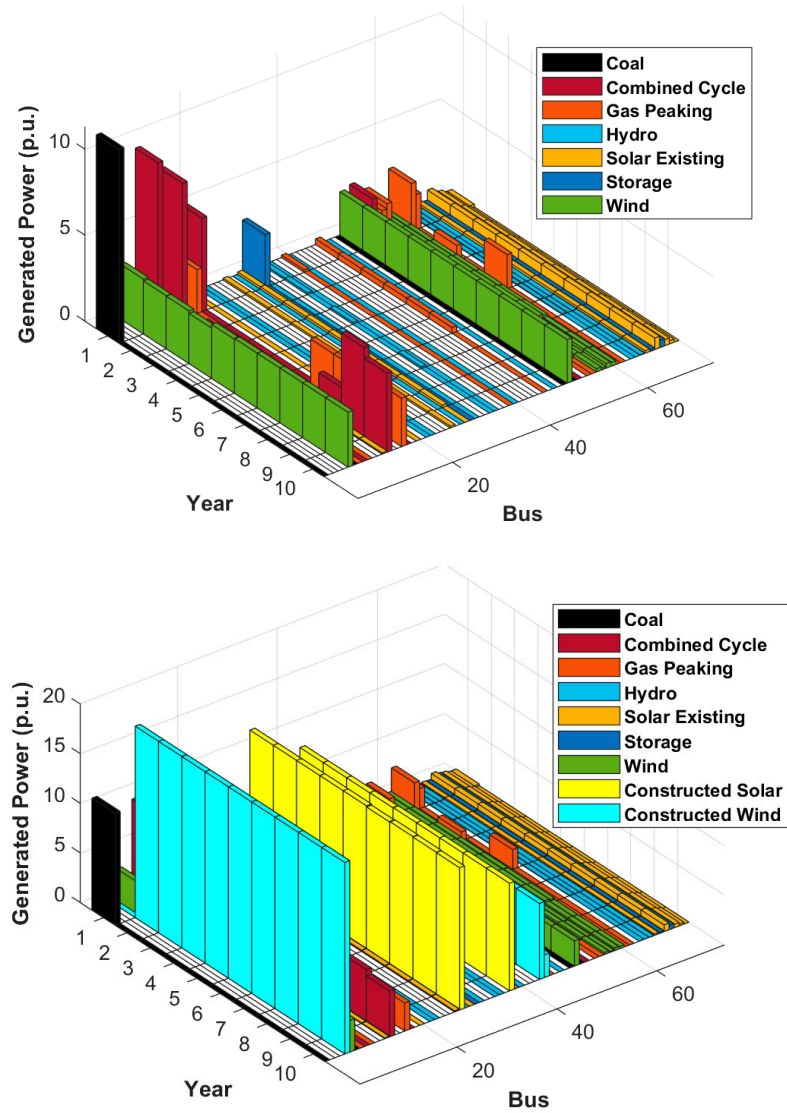
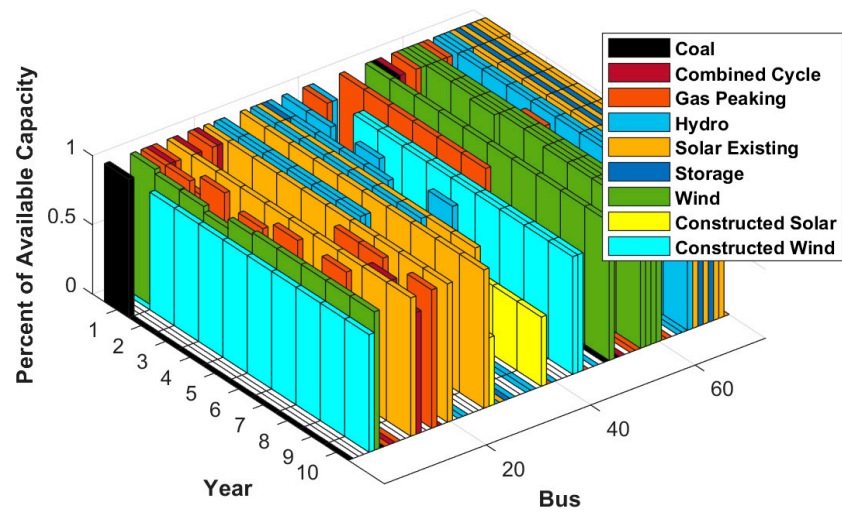


Figure 17. Generation by technology throughout the planning period for the base case.

Figure 19 depicts the operation level of each generation technology as a percentage of its available capacity. It can be seen that many previously existing renewable energy plants are operating at their available capacity. The newly constructed solar plants are not working at their total capacity for this scenario and operating condition. However, the additional capacity is necessary for scenarios 1 through 9 when lines or generators are down but demand must still be served.



**Figure 18.** Generation by source over time—base case, normal (no contingency) operation, and above-average demand. Top: existing generation. Bottom: existing and added generation.



**Figure 19.** Generation levels at different buses as a percentage of the available total capacity—base case, normal (no contingency) operation, and higher-than-average demand.

#### 4.3. Impact of Social Vulnerabilities

As described in Sections 2 and 3, each demand node is assigned a social vulnerability index between 0 and 1, with higher numbers indicating higher vulnerabilities. The assigned weights are shown in Figure 20.

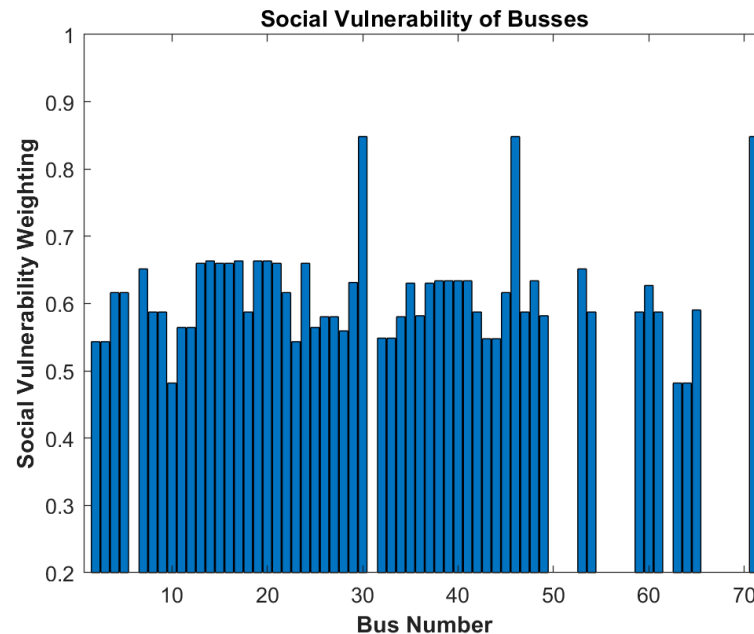
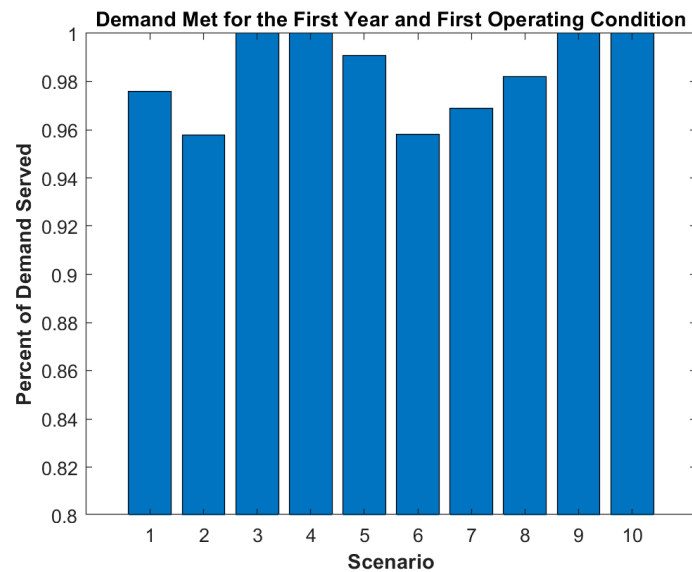


Figure 20. Social vulnerability levels assigned to different demand buses.

For the base case, the entire demand for every scenario and operating condition was met after the initial planning year. However, during year 1 and under certain contingency scenarios, part of the demand was not met because the model was not allowed to add any new generation resources. Figure 21 depicts the amount of demand that was met for each scenario for the first time period and the above-average demand operating condition. Note that scenario 10 represents the normal operation (no contingencies). The entire demand is met here, enforced by constraint (18). However, under contingency scenarios 1, 2, 5, 6, 7, and 8, the network was not able to meet the entire demand. Buses 11, 23, 25, 26, and 65 were all not fully served during various scenarios. Bus 23 was not served for scenarios 1, 2, 6, 7, and 8, which all had downed lines close to or connected to bus 23. Therefore, this bus is predisposed to outages due to wildfires. Bus 26 was also not served for scenario 2 because the transmission line from bus 26 to bus 27 was considered down. In scenario 5, the transmission line between buses 10 and 11 was considered inoperable and had three unserved buses, 11, 25, and 65. The buses with unserved loads (under contingencies) have social vulnerability indices of 0.56, 0.54, 0.56, 0.58, and 0.59. These numbers can be compared with the most socially vulnerable demand buses in the entire network with weightings of 0.85. This indicates that the more socially vulnerable buses in the system were served during all scenarios.

#### 4.4. Discussion

The multi-objective framework proposed in this study ensures that no single objective dominates others and that each objective function is given equal importance. Interestingly, when costs are balanced against life cycle impacts, fossil fuel generation resources are still phased out at the benefit of renewable generation technologies. This might sound counterintuitive; however, it clearly shows that the significant benefits gained from decommissioning those units or reducing their generation levels far outweigh the financial costs associated with deploying new cleaner generation resources.



**Figure 21.** Percentage of demand met for each scenario, for the first year and first operating condition of the base case.

Furthermore, the inclusion of social vulnerability indices in the calculation of energy not served ensures that socially vulnerable populations are given priority during contingencies. This was evident from the results, where the most socially vulnerable buses remained largely unaffected by the wildfire contingency scenarios considered. This underlines that, with equity in mind, the same amount of power can more or less be supplied; however, routed towards those who need it the most, i.e., people and communities who are more affected by the health issues caused by outages, are less prepared for them and/or lack resources to evacuate upon need.

The results show that, assuming that sufficient energy storage can be coupled with renewable resources to maintain real-time stability, Colorado's network can implement a large amount of wind and solar capacity to meet a growing demand. This can be further combined with ambitious decommissioning targets set by the state. The results indicates that the network can potentially serve all loads, even during wildfire scenarios, if more generation capacity is implemented.

#### 4.5. Limitations of the Study

This study does not consider the stochastic and uncertain nature of renewable energy resources such as wind and solar. Realistically, renewable generation may not be as reliable or dispatchable as fossil-fuel-based units. This aspect was modeled in the current work in terms of availability factors for those resources. However, uncertainties can be incorporated into the problem formulation through more advanced stochastic or robust optimization approaches.

Another limitation of the developed model is that the contingencies were incorporated and solved only spatially. The model can be extended to also include temporal variations of natural disasters, e.g., wildfires in this case. This would allow for extending the model to consider more complex ( $N - 1 - m$ ) contingencies that better reflect the dynamics of the event.

Lastly, the case study presented here was developed using publicly available models and data. Although every effort was made to ensure the feasibility of the assumptions and parameters, the results and findings may not be truly reflective of the reality of PSCO's generation and transmission network. A more accurate model for the development of operating conditions, for instance, may affect the solution front of the optimization model.

## 5. Conclusions

Power grid capacity expansion planning has traditionally been modeled as a cost-oriented problem with the goal of minimizing loss of load subject to budgetary constraints. This view fails to see the impact of capacity expansion (or lack thereof) on socially vulnerable populations or the (at times) contradictory interplay between the resilience and sustainability of the power grid. A novel multi-objective optimization framework was proposed in this paper for generation and transmission capacity expansion planning to ensure that a sustainable, equitable, and resilient power grid can be built within a budget. In contrast to the state of the art, where the problem is often viewed merely from financial and technical perspectives, the three objectives of minimizing costs, minimizing energy not served (weighted based on social vulnerabilities of demand areas to long-duration power outages), and minimizing life cycle impacts of different generation and transmission technologies were considered and modeled using a Chebyshev goal programming approach to ensure that no objective dominates others. A realistic case study was built using a part of the bulk power system in the state of Colorado, and various cases such as aggravated load growth and accelerated decommissioning strategies were considered and compared. To model resilience, the risks of outages due to wildfire hazards across the state were modeled in the form of contingency scenarios. The results of the analysis indicated that achieving resilience while ensuring sustainable grid expansion is possible. Furthermore, by including social vulnerabilities in grid expansion, utilities can protect socially vulnerable populations against the dire consequences of natural disasters. The proposed model is generalizable and can be utilized for other generation and transmission networks to assess where more growing networks should focus their efforts first to benefit their populations while being cost-effective and sustainable. The output of the model can provide a tool for policymakers, utilities, and stakeholders to better understand the capital and operational costs of developing a sustainable, resilient, and equitable electric grid.

**Author Contributions:** Conceptualization, S.M.; methodology, S.M. and D.B.; software, D.B.; validation, D.B., P.K. and S.M.; formal analysis, D.B., P.K. and S.M.; investigation, D.B. and S.M.; resources, D.B. and P.K.; data curation, D.B., P.K. and S.M.; writing—original draft preparation, D.B. and S.M.; writing—review and editing, D.B., S.M. and P.K.; visualization, D.B.; supervision, S.M.; project administration, S.M. All authors have read and agreed to the published version of the manuscript.

**Funding:** This research received no external funding.

**Data Availability Statement:** Data used for creating case studies were adopted from publicly available reports [35–42,45].

**Conflicts of Interest:** Author Patrick Kuretich was employed by the company Xcel Energy. The remaining authors declare that the research was conducted in the absence of any commercial or financial relationships that could be construed as a potential conflict of interest.

## Nomenclature

### Indices and Sets

$c$	Index used for life cycle impact category
$C$	Set of impact categories
$d$	Index used for demand
$D$	Set of power system nodes with demand
$g$	Index used for existing generators. These could belong to different technologies, e.g., natural gas, wind farm, nuclear, etc.
$G$	Set of power system nodes with generation
$i$	Index used for nodes of the system
$j$	Index used for nodes of the system
$L$	Set of candidate transmission lines to be installed
$m$	Index used for power system nodes that are candidates for installing a generation resource
$M$	Set of candidate power system nodes for installing a generation resource
$N$	Set of all nodes in the power system

$o$	Index used for operating state of the system
$O$	Set of operating states of the system
$q$	Index used for objective functions within the multi-objective framework
$Q$	Set of objective functions in the multi-objective framework
$s$	Index used for scenarios
$S$	Set of scenarios considered
$S_N$	Set of normal scenarios—a subset of $S$
$t$	Index used for time, i.e., year
$T$	Set of years considered
$tec$	All technologies considered for generation and lines, e.g., solar, wind, etc.
$\varphi$	Commission year
<b>Parameters</b>	
$AV(\cdot)_{t,o,s}$	Availability factor of generation technologies, for thermal units; this is set to 1. This can change depending on the year (for instance, during a drought year), the operating condition (seasonality), and scenarios
$b_{i,j}$	Susceptance of the line connecting nodes $i$ and $j$ [p.u]
$B^{gen}$	Overall budget for installing new generators [USD]
$B^{line}$	Overall budget for installing new lines [USD]
$c_{(\cdot)}^{O\&M}$	Cost of providing power by generator $(\cdot)$ [USD/MW]. Applies to both existing generators $g$ and candidate generators $m$
$c_m^{cap}$	Annualized cost of installing generator $m$ [USD/MW]
$c_{line}$	Annualized cost of setting up a power transmission line between two nodes [\$/km]. Considered to be linearly proportional to the distance between the nodes
$h_{c,tec}^{fixed}$	Fixed environmental impact produced by a specific technology for every impact category considered [environmental impact/functional unit]
$h_{c,tec}^{var}$	Variable environmental impact produced by a specific technology for every impact category considered [environmental impact/functional unit]
$h_o$	Duration of operating state $o$ [hours]. Sum of durations of all operating states should add up to 8760 h
$l_{i,j}$	Length of the line connecting nodes $i$ and $j$ [km]
$p_s$	Probability of occurrence for scenario $s$
$p_{d,t,o,s}^{des}$	Desired demand at node $d$ at year $t$ under operating state $o$ and scenario $s$ [MW]. This could be the peak or the average demand
$p_{i,j,s}^{max}$	Maximum power transfer capacity of the transmission line connecting nodes $i$ and $j$ , under scenario $s$ [MW]. In the most general sense, the index of scenario indicates the changes in line capacity under different contingencies.
$p_{g,s}^{max}$	Maximum capacity of existing generator $g$ under scenario $s$ [MW].
$p_m^{max}$	Rated capacity of potential generator $m$ [MW]. This is the maximum capacity that can be installed at that location and may be limited by financial, geographical, or regulatory constraints
$p_{g,s}^{min}$	Minimum capacity of generator $g$ under scenario $s$ [MW].
$T_q$	Target for objective function $q$ in the multi-objective framework
$\alpha_d$	Social vulnerability level of customers belonging to demand node $d$ —a value between 0 and 1, with higher values indicating higher vulnerabilities
$\eta$	Efficiency factor
$\Lambda$	Lifetime of an asset [hours]
<b>Variables</b>	
$L$	Variable of optimization in the multi-objective framework
$O_q$	Value of objective function $q$ within the multi-objective framework
$p_{d,t,o,s}$	Actual demand at node $d$ at year $t$ under operating state $o$ and scenario $s$ [MW]. This could be the peak or the average demand
$p_{g,t,o,s}$	Power provided by existing generator $g$ at year $t$ under operating state $o$ and scenario $s$ [MW]
$p_{i,j,t,o,s}$	Power flow through the line connecting nodes $i$ and $j$ at year $t$ under operating state $o$ and scenario $s$ [MW]
$p_{m,t}^{max}$	Installed capacity of candidate generator $m$ at year $t$ [MW]

$p_{m,t,o,s}$	Power provided by candidate generator $m$ at year $t$ under operating state $o$ and scenario $s$ [MW]
$s_q$	Deficiency variable for objective function $q$ within the multi-objective framework
$u_{i,j,t}$	Binary variable indicating if candidate transmission line to connect nodes $i$ and $j$ is chosen for deployment at year $t$ (1 = installed, 0 = not installed). Note that this variable is not a function of the operating state, nor a specific scenario, and is instead determined for the entire horizon of the problem while considering all scenarios
$\delta_{i,t,o,s}$	Phase angle at node $i$ at year $t$ under operating state $o$ and scenario $s$ [rad.]

## References

1. Conejo, A.J.; Baringo, L.; Kazempour, S.J.; Siddiqui, A.S. *Investment in Electricity Generation and Transmission*; Springer: Berlin/Heidelberg, Germany, 2016.
2. Meza, J.L.C.; Yildirim, M.B.; Masud, A.S.M. A Model for the Multiperiod Multiobjective Power Generation Expansion Problem. *IEEE Trans. Power Syst.* **2007**, *22*, 871–878. [[CrossRef](#)]
3. Arabali, A.; Ghofrani, M.; Etezadi-Amoli, M.; Fadali, M.S.; Moeini-Aghtaie, M. A Multi-Objective Transmission Expansion Planning Framework in Deregulated Power Systems with Wind Generation. *IEEE Trans. Power Syst.* **2014**, *29*, 3003–3011. [[CrossRef](#)]
4. Sepasian, M.S.; Seifi, H.; Foroud, A.A.; Hatami, A.R. A Multiyear Security Constrained Hybrid Generation-Transmission Expansion Planning Algorithm Including Fuel Supply Costs. *IEEE Trans. Power Syst.* **2009**, *24*, 1609–1618. [[CrossRef](#)]
5. Baringo, L.; Baringo, A. A Stochastic Adaptive Robust Optimization Approach for the Generation and Transmission Expansion Planning. *IEEE Trans. Power Syst.* **2018**, *33*, 792–802. [[CrossRef](#)]
6. Pozo, D.; Sauma, E.E.; Contreras, J. A Three-Level Static MILP Model for Generation and Transmission Expansion Planning. *IEEE Trans. Power Syst.* **2013**, *28*, 202–210. [[CrossRef](#)]
7. Yao, F.; Chau, T.K.; Zhang, X.; Iu, H.H.-C.; Fernando, T. An Integrated Transmission Expansion and Sectionalizing-Based Black Start Allocation of BESS Planning Strategy for Enhanced Power Grid Resilience. *IEEE Access* **2020**, *8*, 148968–148979. [[CrossRef](#)]
8. Gu, Y.; McCalley, J.D.; Ni, M. Coordinating Large-Scale Wind Integration and Transmission Planning. *IEEE Trans. Sustain. Energy* **2012**, *3*, 652–659. [[CrossRef](#)]
9. Khodaei, A.; Shahidehpour, M.; Wu, L.; Li, Z. Coordination of Short-Term Operation Constraints in Multi-Area Expansion Planning. *IEEE Trans. Power Syst.* **2012**, *27*, 2242–2250. [[CrossRef](#)]
10. Aghaei, J.; Amjadi, N.; Baharvandi, A.; Akbari, M.-A. Generation and Transmission Expansion Planning: MILP-Based Probabilistic Model. *IEEE Trans. Power Syst.* **2014**, *29*, 1592–1601. [[CrossRef](#)]
11. Yin, S.; Wang, J. Generation and Transmission Expansion Planning towards a 100% Renewable Future. *IEEE Trans. Power Syst.* **2022**, *37*, 3274–3285. [[CrossRef](#)]
12. López, J.Á.; Ponnambalam, K.; Quintana, V.H. Generation and Transmission Expansion Under Risk Using Stochastic Programming. *IEEE Trans. Power Syst.* **2007**, *22*, 1369–1378. [[CrossRef](#)]
13. Muñoz-Delgado, G.; Contreras, J.; Arroyo, J.M.; de la Nieta, A.S.; Gibescu, M. Integrated Transmission and Distribution System Expansion Planning Under Uncertainty. *IEEE Trans. Smart Grid* **2021**, *12*, 4113–4125. [[CrossRef](#)]
14. Mavalizadeh, H.; Ahmadi, A.; Gandoman, F.H.; Siano, P.; Shayanfar, H.A. Multiobjective Robust Power System Expansion Planning Considering Generation Units Retirement. *IEEE Syst. J.* **2018**, *12*, 2664–2675. [[CrossRef](#)]
15. Moreira, A.; Pozo, D.; Street, A.; Sauma, E. Reliable Renewable Generation and Transmission Expansion Planning: Co-Optimizing System's Resources for Meeting Renewable Targets. *IEEE Trans. Power Syst.* **2017**, *32*, 3246–3257. [[CrossRef](#)]
16. Shu, J.; Wu, L.; Zhang, L.; Han, B. Spatial Power Network Expansion Planning Considering Generation Expansion. *IEEE Trans. Power Syst.* **2015**, *30*, 1815–1824. [[CrossRef](#)]
17. Romero, N.R.; Nozick, L.K.; Dobson, I.D.; Xu, N.; Jones, D.A. Transmission and Generation Expansion to Mitigate Seismic Risk. *IEEE Trans. Power Syst.* **2013**, *28*, 3692–3701. [[CrossRef](#)]
18. Li, J.; Li, Z.; Liu, F.; Ye, H.; Zhang, X.; Mei, S.; Chang, N. Robust Coordinated Transmission and Generation Expansion Planning Considering Ramping Requirements and Construction Periods. *IEEE Trans. Power Syst.* **2018**, *33*, 268–280. [[CrossRef](#)]
19. Byles, D.; Mohagheghi, S. Sustainable Power Grid Expansion: Life Cycle Assessment, Modeling Approaches, Challenges, and Opportunities. *Sustainability* **2023**, *15*, 8788. [[CrossRef](#)]
20. Federal Energy Regulatory Commission. Grid Reliability and Resilience Pricing, Docket No. RM18-1-000. Available online: <https://www.ferc.gov/media/grid-reliability-and-resilience-pricing-docket-no-rm18-1-000> (accessed on 17 December 2023).
21. Daeli, A.; Mohagheghi, S. Power Grid Infrastructural Resilience against Extreme Events. *Energies* **2023**, *16*, 64. [[CrossRef](#)]
22. Defining Power System Resilience. CIGRE. Available online: <https://www.cigre.org/article//defining-power-system-resilience> (accessed on 17 December 2023).
23. Yuan, H.; Zhang, W.; Zhu, J.; Bagtzoglou, A.C. Resilience Assessment of Overhead Power Distribution Systems under Strong Winds for Hardening Prioritization. *ASCE-ASME J. Risk Uncertain. Eng. Syst. Part A Civ. Eng.* **2018**, *4*, 04018037. [[CrossRef](#)]
24. Dugan, J.; Byles, D.; Mohagheghi, S. Social vulnerability to long-duration power outages. *Int. J. Disaster Risk Reduct.* **2023**, *85*, 103501. [[CrossRef](#)]
25. Liu, X.; Xu, Z.; Gou, X.; Xiao, J.; Zhao, Y. A decision-making model for efficient fair electricity rationing under major power outage emergencies. *Int. J. Comput. Commun. Control* **2023**, *18*, 5554. [[CrossRef](#)]

26. Bharati, A.K.; Singhal, A.; Jinsiwale, R.; Kazimierczuk, K.; Yoshimura, J.; Tarekegne, B. Advancing Energy Equity Considerations in Distribution Systems Planning. In Proceedings of the 2023 IEEE Power & Energy Society Innovative Smart Grid Technologies Conference (ISGT), Washington, DC, USA, 16–19 January 2023; pp. 1–5. [CrossRef]
27. Rodriguez-Garcia, L.; Hassan, A.; Parvania, M. Equity-aware power distribution system restoration. *IET Gener. Transm. Distrib.* **2023**, *18*, 401–412. [CrossRef]
28. Montoya-Rincon, J.P.; Mejia-Manrique, S.A.; Azad, S.; Ghandehari, M.; Harmsen, E.W.; Khanbilvardi, R.; Gonzalez-Cruz, J.E. A socio-technical approach for the assessment of critical infrastructure system vulnerability in extreme weather events. *Nat. Energy* **2023**, *8*, 1002–1012. [CrossRef]
29. Gunda, T.; Wachtel, A.; Mishra, S.K.; Moog, E. Quantitative approaches for including equity in risk and resilience infrastructure planning analyses. *Risk Anal.* **2023**, 1–12. [CrossRef] [PubMed]
30. National Renewable Energy Laboratory. ATB|NREL. Annual Technology Baseline. Available online: <https://atb.nrel.gov/> (accessed on 17 December 2023).
31. Rauner, S.; Budzinski, M. Holistic energy system modeling combining multi-objective optimization and life cycle assessment. *Environ. Res. Lett.* **2017**, *12*, 124005. [CrossRef]
32. Huijbregts, M.A.J.; Steinmann, Z.J.N.; Elshout, P.M.F.; Stam, G.; Verones, F.; Vieira, M.; Zijp, M.; Hollander, A.; van Zelm, R. ReCiPe2016: A harmonised life cycle impact assessment method at midpoint and endpoint level. *Int. J. Life Cycle Assess.* **2017**, *22*, 138–147. [CrossRef]
33. OpenLCA. Available online: <https://www.openlca.org/> (accessed on 17 December 2023).
34. Li, C.; Conejo, A.J.; Liu, P.; Omell, B.P.; Sirola, J.D.; Grossmann, I.E. Mixed-integer linear programming models and algorithms for generation and transmission expansion planning of power systems. *Eur. J. Oper. Res.* **2022**, *297*, 1071–1082. [CrossRef]
35. 2021 Electric Resource Plan & Clean Energy Plan; Progress Report 21A-0141E; Xcel Energy: Minneapolis, MN, USA, 2023.
36. 2021 Electric Resource Plan and Clean Energy Plan; Technical Appendix 21A-E; Public Service Company of Colorado: Denver, CO, USA, 2021.
37. Substations, J.L. 2021. Available online: [https://services1.arcgis.com/CD5mKowwN6n1aqd8/arcgis/rest/services/Infrastructure\\_HVRA\\_Source\\_Data\\_Substations/FeatureServer](https://services1.arcgis.com/CD5mKowwN6n1aqd8/arcgis/rest/services/Infrastructure_HVRA_Source_Data_Substations/FeatureServer) (accessed on 13 February 2024).
38. Xcel Energy. 3727 Stakeholder Meeting. 13 December 2022. Available online: [https://www.transmission.xcelenergy.com/staticfiles/microsites/Transmission/Files/FERC\\_890\\_Q4\\_2022\\_12-13-22\\_Final.pdf](https://www.transmission.xcelenergy.com/staticfiles/microsites/Transmission/Files/FERC_890_Q4_2022_12-13-22_Final.pdf) (accessed on 17 December 2023).
39. Power Plants in the US (FeatureServer). Available online: [https://services2.arcgis.com/FiaPA4ga0iQKduv3/arcgis/rest/services/Power\\_Plants\\_in\\_the\\_US/FeatureServer](https://services2.arcgis.com/FiaPA4ga0iQKduv3/arcgis/rest/services/Power_Plants_in_the_US/FeatureServer) (accessed on 17 December 2023).
40. Transmission Lines. Available online: <https://hifld-geoplatform.opendata.arcgis.com/datasets/transmission-lines/> (accessed on 17 December 2023).
41. Building An Open Guide to the World’s Energy System. Global Energy Monitor. Available online: <https://globalenergymonitor.org/> (accessed on 17 December 2023).
42. West Station-Greenhorn 115 kV Line Rebuild; Appendix 21M-0005E. Black Hills Colorado Electric: Arkansas, CO, USA, 2018. Available online: <https://www.blackhillsenergy.com/sites/blackhillsenergy.com/files/coe-west-station-greenhorn-115-kv-line-rebuild.pdf> (accessed on 17 December 2023).
43. 230 kV Specifications. BOLD Transmission. 2017. Available online: <https://www.boldtransmission.com/wp-content/uploads/2018/04/BOLD-230-kV-Specifications.pdf> (accessed on 17 December 2023).
44. Berger, D. *Pawnee-Smoky Hill 345 kV Conductor Comparison*; Senate Bill, Xcel Energy: Minneapolis, MN, USA, 2008.
45. *Electric Quality of Service Plan 2021 Annual Summary Report*; Xcel Energy: Minneapolis, MN, USA, April 2021.
46. C.S.D. Office. Population Totals Counties. Available online: [https://demography.dola.colorado.gov/assets/lookups/county\\_totop\\_lookup.html](https://demography.dola.colorado.gov/assets/lookups/county_totop_lookup.html) (accessed on 17 December 2023).
47. Office of Energy Efficiency and Renewable Energy. Wind Energy in Colorado. WINDEXchange. Available online: <https://windexchange.energy.gov/states/co> (accessed on 17 December 2023).
48. National Renewable Energy Laboratory. Solar Resource Maps and Data. Geospatial Data Science. Available online: <https://www.nrel.gov/gis/solar-resource-maps.html> (accessed on 17 December 2023).
49. Project Description. Xcel Energy Colorado Power Pathway. Available online: <https://www.coloradospowerpathway.com/project-description/> (accessed on 17 December 2023).
50. Hourly Electric Grid Monitor. U.S. Energy Information Administration. Available online: <https://www.eia.gov/electricity/gridmonitor/index.php> (accessed on 17 December 2023).
51. RDW\_Wildfire/RMRS\_WRC\_BurnProbability (ImageServer). Available online: [https://apps.fs.usda.gov/fsgisx01/rest/services/RDW\\_Wildfire/RMRS\\_WRC\\_BurnProbability/ImageServer](https://apps.fs.usda.gov/fsgisx01/rest/services/RDW_Wildfire/RMRS_WRC_BurnProbability/ImageServer) (accessed on 17 December 2023).
52. Scott, J.H.; Thompson, M.P.; Calkin, D.E. *A Wildfire Risk Assessment Framework for Land and Resource Management*; General Technical Report RMRS-GTR-315. U.S.; Department of Agriculture, Forest Service, Rocky Mountain Research Station: Fort Collins, CO, USA, 2013; 83p.

**Disclaimer/Publisher’s Note:** The statements, opinions and data contained in all publications are solely those of the individual author(s) and contributor(s) and not of MDPI and/or the editor(s). MDPI and/or the editor(s) disclaim responsibility for any injury to people or property resulting from any ideas, methods, instructions or products referred to in the content.